

Polarization and Polarimetry of ^3He

A thesis submitted in partial fulfillment of the requirement
for the degree of Bachelor of Science with Honors in
Physics from the College of William and Mary in Virginia,

by

Daniel Edward Milkie

Accepted for _____
(Honors, High Honors, or Highest Honors)

Advisor: Dr. Todd D. Averett

Dr. Morton Eckhouse

Dr. Keith A. Griffioen

Dr. Gina L. Hoatson

Dr. George T. Rublein

Williamsburg, Virginia
April 2002

ABSTRACT

Nuclear physics experiments probe the internal structure of the neutron using electron scattering from polarized ^3He targets. At the College of William and Mary, a lab has been constructed for polarizing ^3He and for polarimetry measurements. Polarization of ^3He occurs during spin-exchange collisions with optically pumped, polarized Rb atoms. Polarization is measured using nuclear magnetic resonance and the adiabatic fast passage technique. Descriptions of the experimental system and results are presented here.

ACKNOWLEDGEMENTS

I would like to thank all of those who supported me in this research. I want to give special thanks to Kevin Kramer for his help with LabView and the NMR system, Vincent Sulkosky for his experience in NMR and with the optics, and Tamara Hayford who developed the oven and was great to work alongside in all aspects of the lab. Finally, I would like to especially thank Dr. Todd Averett who fueled my excitement and passion for physics throughout this honors research. His commitment to his students and this project made this work a success.

CONTENTS

Abstract.....	ii
Acknowledgements.....	iii
1. Introduction.....	1
2. Polarization Processes.....	4
2.1 Optical Pumping.....	4
2.2 Helium-3 Polarization by Spin Exchange.....	6
2.3 Factors Increasing Polarization.....	7
2.4 Factors Decreasing Polarization.....	7
3. Polarimetry Theory.....	9
3.1 Energy of a Magnetic Moment in a Magnetic Field.....	9
3.2 Precession in a Magnetic Field.....	10
3.3 The Case of Static and Rotating Fields.....	12
3.4 The Case of Static and Oscillating Fields.....	13
3.5 Conditions of Adiabatic Fast Passage.....	15
4. Experimental Setup.....	18
4.1 Magnetic Coils and Electronics.....	18
4.2 Target Cell and Oven.....	25
4.3 Laser and Optics.....	26
5. Experimental Procedures.....	28
5.1 Pickup Coil Alignment.....	28
5.2 Q-Factor of the Pickup Coil Circuit.....	30
5.3 Laser Tuning.....	31
5.4 Polarization	32
5.5 Polarimetry.....	33
6. Conclusions and Future Research	34
A. Software Documentation.....	36
A1. “NMR Q Curve WM.vi”.....	36
A2. “NMR Load Sweep.vi”.....	38
A3. “NMR Helium XY FG-V WM.vi”.....	41

A4. “AGLIENT LOAD WAVEFORM.vi”.....	43
B. Pictures.....	46
References.....	50

1. INTRODUCTION

The theory of quantum chromodynamics is used to explain the substructure of the neutron[1,2]. Scattering experiments with polarized (spin-aligned) electron beams and polarized targets test this theory by studying the quark structure of the neutron. Ideally, polarized neutron targets would be used in scattering experiments, but a free neutron has a half-life of 10.23 minutes[3]. A stable alternative to a free neutron is a ${}^3\text{He}$ nucleus.

In the ${}^3\text{He}$ ground state, the nucleus is predominantly in the S-state from which the spins of the two protons are anti-aligned. This configuration effectively cancels the proton spin contribution to the nuclear magnetic moment[4]. Thus, with slight corrections for residual proton effects[5], the ${}^3\text{He}$ nuclear spin is dominated by that of the neutron. Scattering experiments[6,7,8,9,10] that study neutron spin structure therefore often use polarized ${}^3\text{He}$ targets.

At the College of William and Mary, aluminosilicate glass target cells (Fig. 1) are filled with 8.5 amagats (1 amagat of gas = 1 atm of gas at room temperature) of ${}^3\text{He}$ for experiments at the Thomas Jefferson National Accelerator Facility (Jefferson Lab). At Jefferson Lab, the ${}^3\text{He}$ target is polarized and placed in a high-energy, polarized electron beam. As the electrons pass through the target cell, they scatter from the polarized ${}^3\text{He}$ nuclei. Using detectors these scattering events are measured. Experiments using these targets achieve a statistical error that is inversely proportional to the square of the target polarization for a fixed amount of beam time. Recent experiments at Jefferson Lab show that the current targets achieve, on average, a ${}^3\text{He}$ polarization of about 40%[11]. With higher ${}^3\text{He}$ polarization, results could be obtained with much greater precision or in a shorter running time.

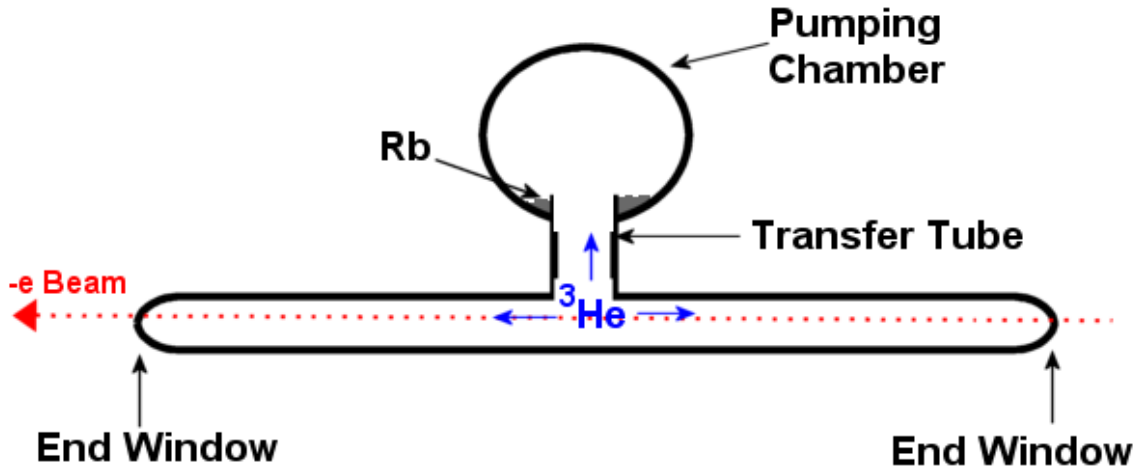


Figure 1: Schematic of a ${}^3\text{He}$ target cell. A glass lip holds a small amount of rubidium (Rb) in the pumping chamber. The transfer tube allows ${}^3\text{He}$ to flow between the chambers. The electron beam is used during scattering experiments at Jefferson Lab.

The goal of this research was to construct a facility at the College of William and Mary for the polarization of ${}^3\text{He}$ and for polarimetry measurements. This facility enables future investigations to improve target performance. The apparatus (Fig. 2) primarily consists of optical pumping equipment (laser and optics) for polarizing ${}^3\text{He}$ and a nuclear magnetic resonance system (three pairs of coils) for adiabatic fast passage polarimetry experiments.

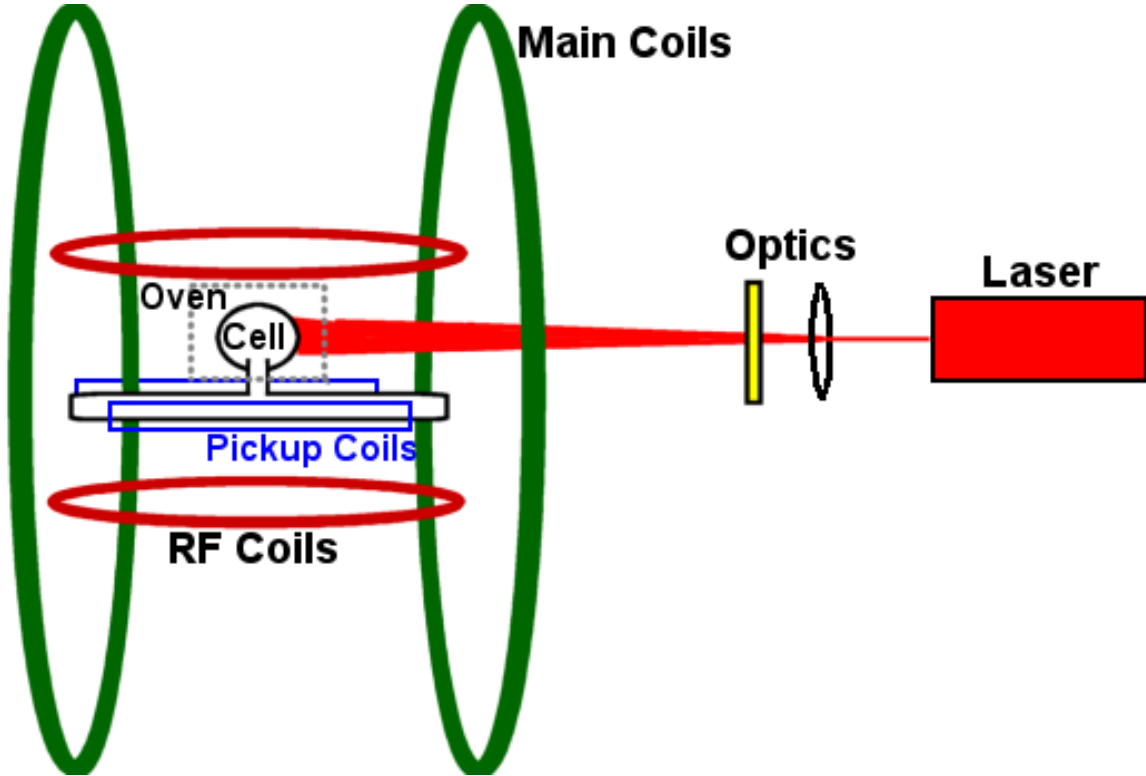


Figure 2: Schematic of the apparatus for polarization and polarimetry of ${}^3\text{He}$. The laser, main coils, optics, and oven are used in optical pumping. The main coils, the RF coils, and the pickup coils are used in determining the ${}^3\text{He}$ polarization.

The use of polarized ${}^3\text{He}$ extends beyond nuclear physics experiments into other fields including medical diagnostics. At the University of Virginia and other research labs[12,13,14] adaptations of techniques described in this thesis have been successful in the investigation of lung spaces. In the human lung, a lack of hydrogen prevents effective traditional magnetic resonance imaging (MRI). By inhaling a polarized noble gas, the MRI is enhanced and produces temporally and spatially precise scans (Fig. 3) without the use of harmful radioactive tracers. This enhancement[15] is due to the polarized noble gas's large magnetic moment.

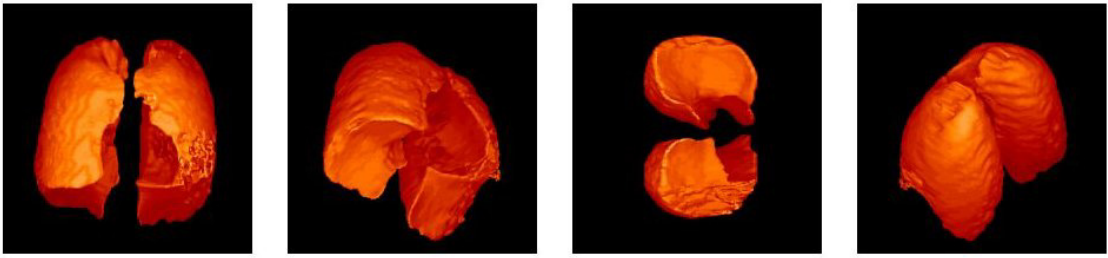


Figure 3: A 3D MRI rendering of human lungs using inhaled polarized ${}^3\text{He}$ [16].

2. POLARIZATION PROCESSES

Polarization P is defined as

$$P = \frac{N^\uparrow - N^\downarrow}{N^\uparrow + N^\downarrow} \quad (1)$$

where N^\uparrow is the number of spins aligned and N^\downarrow is the number of spins anti-aligned with a magnetic (holding) field (quantization axis). In this lab, ${}^3\text{He}$ is polarized using a two-part process. First, rubidium (Rb) vapor in the pumping chamber of the target cell is atomically polarized through optical pumping. The Rb polarization is then transferred to the ${}^3\text{He}$ nuclei by spin-exchange collisions.

2.1 OPTICAL PUMPING

Rubidium is an alkali metal, whose polarization is determined by the spin state of its single valence electron. A magnetic holding field \vec{H}_0 (produced by the main coils) is used to separate and distinguish the otherwise spin-degenerate energy states. As shown in Fig. 4, the Zeeman effect splits the ground state of Rb into the $5\text{S}_{1/2}$ $m = -1/2$ and $5\text{S}_{1/2}$ $m = +1/2$ states and the first excited state into the $5\text{P}_{1/2}$ $m = -1/2$ and $5\text{P}_{1/2}$ $m = +1/2$ states (with the hyperfine splitting ignored). Due to selection rules, photons

propagating along the direction of the magnetic field, of positive helicity $\sigma+$, and of wavelength 795 nm will excite only electrons from the $5S_{1/2}$ $m = -1/2$ state to the $5P_{1/2}$ $m = +1/2$ state. Collisions between Rb atoms quickly distribute $5P_{1/2}$ $m = +1/2$ electrons between both $5P_{1/2}$ spin states. From the excited $5P_{1/2}$ states, decay is equally probable to either $5S_{1/2}$ ground state with $m = -1/2$ (to be excited again) or $m = +1/2$ (the desired polarization). With continuous pumping, the $5S_{1/2}$ $m = +1/2$ state quickly populates to a very high percentage[17].

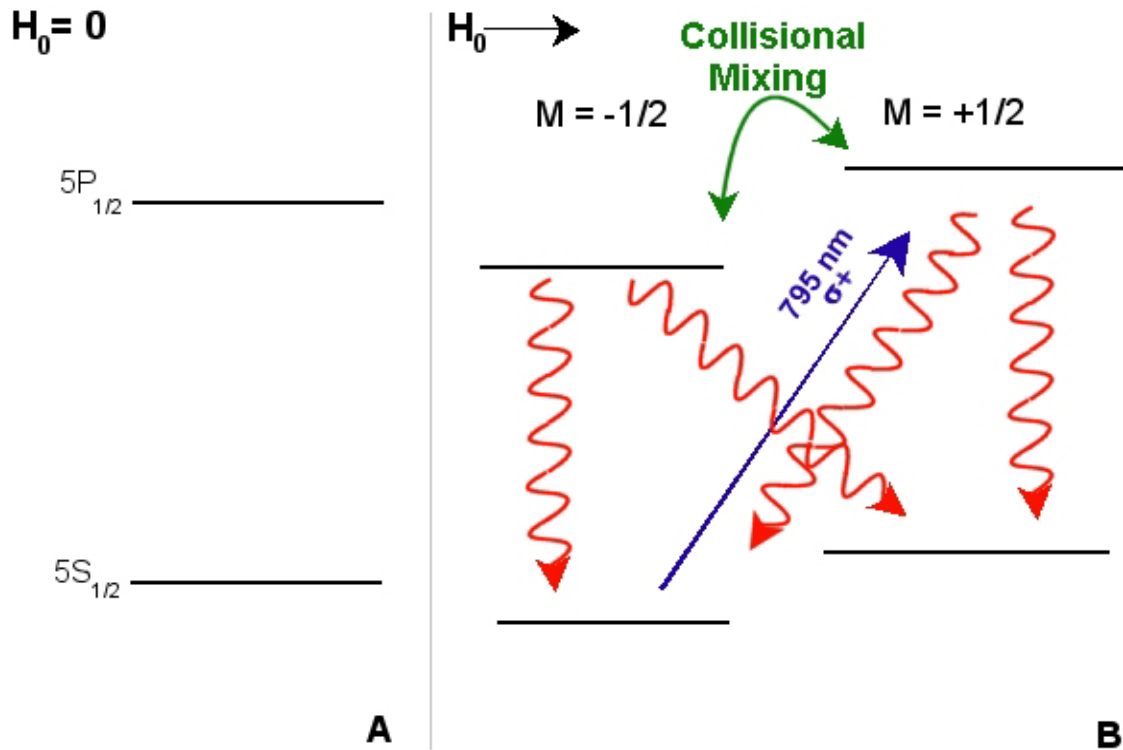


Figure 4: The Rb energy states without a magnetic field (A) and the Zeeman splitting of the Rb energy states due to a magnetic field H_0 (B) from the main coils. The excitation from the $5S_{1/2}$ $m = -1/2$ state (straight arrow), the collisional mixing which redistributes excited electrons (curved arrow), and the decays back to the ground state (wavy arrows) are the processes of optical pumping.

Optical pumping loses effectiveness to polarized Rb if radiative decays from the excited state ($5P_{1/2}$) to the ground state ($5S_{1/2}$) occur. Due to the high density of Rb vapor

in the pumping chamber, an emitted photon has a mean free path many times shorter than size of the pumping chamber and is therefore very likely to be re-absorbed. A photon emitted from a $5P_{1/2}$ - $5S_{1/2}$ decay has a wavelength of 795nm but an undetermined polarization or direction of propagation. This photon is capable of exciting a Rb atom out of the desired $5S_{1/2}$ $m = +1/2$ state. To prevent radiative decays, a small amount of N₂ (about 60 torr at room temperature) was added to the target cell during filling. Diatomic nitrogen is a molecule with numerous rotational and vibrational modes that easily absorb the energy of de-exciting Rb atoms[18]. Through collisions, the N₂ quenches the excited Rb back to the ground state without allowing the Rb to emit depolarizing radiation.

2.2 HELIUM-3 POLARIZATION BY SPIN EXCHANGE

The Rb atomic polarization is transferred to the ^3He nuclei through spin-exchange collisions. In binary collisions between Rb and ^3He , a hyperfine-like interaction can transfer the spin of the Rb atom to the spin of the ^3He nucleus[19]. Since the Rb has been optically pumped to the $m = +1/2$ state, this process can transfer only +1 angular momentum to a ^3He nucleus in the $m = -1/2$ state. After spin exchange, the Rb atom is in the $m = -1/2$ state (to be optically pumped again), and the ^3He nucleus is in $m = +1/2$ state (the desired polarization). The rate of polarization of the ^3He is:

$$\frac{dP_{\text{He}}(t)}{dt} = \gamma_{SE} [\langle P_{Rb} \rangle - P_{\text{He}}(t)] - \Gamma P_{\text{He}}(t) \quad (2)$$

in which P_{He} is the ^3He polarization, γ_{SE} is the rate of spin exchange between Rb and ^3He , $\langle P_{Rb} \rangle$ is the average Rb polarization, and Γ is the total depolarization rate. Solving this differential for P_{He} gives

$$P_{He}(t) = \frac{\gamma_{SE}}{\gamma_{SE} + \Gamma} \langle P_{Rb} \rangle \left(1 - e^{-(\gamma_{SE} + \Gamma)t} \right) \quad (3)$$

In the limit of large time, Eq. 3 becomes:

$$P_{He}^{Final} = \frac{\gamma_{SE}}{\gamma_{SE} + \Gamma} \langle P_{Rb} \rangle \quad (4)$$

With $\langle P_{Rb} \rangle$ maximized by continuous optical pumping, it is evident from Eq. 4 that an increase in ${}^3\text{He}$ polarization is achieved only by increasing γ_{SE} or decreasing Γ .

2.3 FACTORS INCREASING POLARIZATION

The spin exchange rate γ_{SE} is described by

$$\gamma_{SE} \propto k_{SE} [Rb] \quad (5)$$

If it is assumed that the probability of spin-exchange k_{SE} is constant, γ_{SE} can only increase only by raising the Rb vapor concentration $[Rb]$ in the cell. At very high densities, however, the Rb vapor becomes optically opaque which prevents uniform absorption of the circularly polarized light needed for Rb optical pumping. With the present setup, it has been found experimentally that the optimum Rb density occurs at about 170°C.

2.4 FACTORS DECREASING POLARIZATION

The depolarization rate Γ can be expressed as the inverse of a relaxation time $T = 1/\Gamma$. The following factors contribute to shortening T :

- 1) ${}^3\text{He}$ collisions with cell wall paramagnetic impurities. Microfissures in the cell

walls increase the number of collisions by increasing surface area and trapping ^3He atoms. (typical Jefferson Lab target cell $T \approx 80$ hours)

2) Magnetic dipole-dipole interactions between ^3He nuclei[20] (for a typical Jefferson Lab target cell $T \approx 84$ hours)

3) Ionization from experimental electron beam[21-23] (for a $10 \mu\text{A}$ beam, $T \approx 30$ hours[24])

4) Magnetic holding field gradients[25-26] (coils of 1.0 m diameter give $T \approx 1000$ hours)

5) Interactions with gas impurities (T depends on the impurity types and concentrations, but usually not significantly)

For a good cell, the typical lifetime is about 50 hours. Factors 1,4 and 5 are effects of laboratory conditions. Cell wall collisions, is inherently related to cell construction and design. Potential improvements include using a cell wall coating[27], a new cell shape, other types of glasses, a different cell filling procedure, or an entirely new cell wall material. This lab will allow experiments to test these possibilities.

3. POLARIMETRY THEORY

Nuclear magnetic resonance (NMR) is used to measure the ${}^3\text{He}$ polarization using a technique called adiabatic fast passage (AFP)[28]. This process involves manipulating the ${}^3\text{He}$ nuclear spin using time-dependent magnetic fields. First, the energy of a magnetic moment (${}^3\text{He}$ nucleus) in a magnetic field will be discussed. It will be shown that a magnetic moment precesses about the magnetic field at a specific frequency (the Larmor frequency). The effect of adding a rotating magnetic field will then be detailed, and the resonance condition will be found. Next, it will be explained how a rotating magnetic field is obtained in practice. Finally, the conditions for adiabatic fast passage and the effect of passing through resonance will be derived.

3.1 ENERGY OF A MAGNETIC MOMENT IN A MAGNETIC FIELD

The magnetic moment of a nucleus is defined as

$$\vec{\mu} \equiv \gamma \hbar \vec{J} \quad (6)$$

Here, γ is the gyromagnetic ratio (a constant particular for each nucleus with the units $\frac{1}{\text{s}\bullet\text{G}}$), and $\hbar \vec{J}$ is the total angular momentum (the vector sum of the spin and orbital angular momenta of the nucleus). It is well known that the energy E of a magnetic moment $\vec{\mu}$ in a magnetic field \vec{H} is

$$E = -\vec{\mu} \bullet \vec{H} \quad (7)$$

By choosing the quantization axis \hat{z} aligned with the magnetic field $\vec{H} = H\hat{z}$, Eq. 6 and Eq. 7 are combined to establish the nuclear spin energy eigenstates

$$E = -\gamma \hbar \vec{H} \bullet \vec{J} = -\gamma \hbar H J_z \quad (8)$$

where J_z is the component of total angular momentum along \hat{z} and has eigenvalues $(-J, -J+1, \dots, J-1, J)$. The energy difference between neighboring ($\Delta J_z = \pm 1$) eigenstates is

$$\Delta E = \gamma \hbar H \quad (9)$$

This energy corresponds to that of the photon that is emitted or absorbed during a transition between the two states. For a nucleus with gyromagnetic ratio γ in a magnetic field H , the photon frequency necessary for transitions between energy levels is

$$\omega = \gamma H \quad (10)$$

3.2 PRECESSION IN A MAGNETIC FIELD

A nucleus of magnetic moment $\vec{\mu}$ in a magnetic field \vec{H} experiences a torque

$$\vec{N} = \vec{\mu} \times \vec{H} \quad (11)$$

A torque produces a change in angular momentum. Eq. 11 therefore can be rewritten as

$$\frac{d(\hbar \vec{J})}{dt} = \vec{\mu} \times \vec{H} \quad (12)$$

By substituting for $\hbar \vec{J}$ using Eq. 6, Eq. 12 becomes

$$\frac{d(\vec{\mu})}{dt} = \gamma (\vec{\mu} \times \vec{H}) \quad (13)$$

The transformation of the time derivative $\frac{d\vec{V}(t)}{dt}$ of any time-dependent vector $\vec{V}(t)$ to its time derivative $\frac{\delta \vec{V}(t)}{\delta t}$ in a frame rotating at an angular frequency $\vec{\omega}'$ is given by

$$\frac{d\vec{V}(t)}{dt} = \frac{\delta\vec{V}(t)}{\delta t} + \bar{\omega}' \times \vec{V}(t) \quad (14)$$

Transforming Eq. 13 to a frame S' rotating at the angular frequency $\bar{\omega}'$ gives

$$\frac{\delta(\bar{\mu})}{\delta t} + \bar{\omega}' \times \bar{\mu} = \gamma(\bar{\mu} \times \bar{H}) \quad (15)$$

Simplifying Eq. 15 gives

$$\frac{\delta(\bar{\mu})}{\delta t} = \gamma \left(\bar{\mu} \times (\bar{H} + \frac{\bar{\omega}'}{\gamma}) \right) \quad (16)$$

The direction of the frame rotation is chosen to be counter-clockwise when viewed in the direction of the magnetic field (the $+\hat{H}$ direction). In other words, $\bar{\omega}' = \omega'(-\hat{H})$. Eq. 16 can now be rewritten as

$$\frac{\delta(\bar{\mu})}{\delta t} = \gamma \left(\bar{\mu} \times (H - \frac{\omega'}{\gamma}) \hat{H} \right) \quad (17)$$

If the frame rotates at an angular frequency $\omega' = \gamma H$, the torque experienced by the magnetic moment will be

$$\frac{\delta(\bar{\mu})}{\delta t} = \gamma(\bar{\mu} \times 0) = 0 \quad (18)$$

Eq. 18 shows that the magnitude and direction of $\bar{\mu}$ in this frame is constant. In the lab frame, this is interpreted as a precession of $\bar{\mu}$ about \hat{H} with frequency ω' . The angular frequency of precession ω' about a field H is known as the Larmor frequency. It is interesting to note that this frequency $\omega' = \gamma H$ is identical to the photon frequency (Eq. 10) needed to stimulate energy-level transitions.

3.3 THE CASE OF STATIC AND ROTATING FIELDS

Now the case of a magnetic moment in a magnetic field with a rotating component $H_1[\cos(\omega_l t)\hat{x} - \sin(\omega_l t)\hat{y}]$ and a static component $H_0\hat{z}$ will be considered (Fig. 5). To move to a reference frame rotating at $\vec{\omega}_l = -\omega_l\hat{z}$, the transformations

$$\begin{aligned}\hat{z}' &= \hat{z} \\ \hat{x}' &= \cos(\omega_l t)\hat{x} - \sin(\omega_l t)\hat{y} \\ \hat{y}' &= \cos(\omega_l t)\hat{y} + \sin(\omega_l t)\hat{x}\end{aligned}\tag{19}$$

are made. In this rotating frame, the combined magnetic field is $\vec{H}' = H_0\hat{z}' + H_1\hat{x}'$, and the change in magnetic moment (using Eq. 16) is

$$\frac{\delta(\bar{\mu})}{\delta t} = \gamma \left(\bar{\mu} \times \left[H_0\hat{z}' + H_1\hat{x}' + \frac{\vec{\omega}_l}{\gamma} \right] \right)\tag{20}$$

Grouping like terms gives

$$\frac{\delta(\bar{\mu})}{\delta t} = \gamma \left(\bar{\mu} \times \left[\left(H_0 - \frac{\omega_l}{\gamma} \right) \hat{z}' + H_1 \hat{x}' \right] \right)\tag{21}$$

An effective magnetic field (Fig. 5)

$$\vec{H}_{eff} \equiv \left(H_0 - \frac{\omega_l}{\gamma} \right) \hat{z}' + H_1 \hat{x}'\tag{22}$$

can now be used to simplify Eq. 21 to

$$\frac{\delta(\bar{\mu})}{\delta t} = \gamma \left(\bar{\mu} \times \vec{H}_{eff} \right)\tag{23}$$

Eq. 23 is the rotating frame equivalent of Eq. 13 with $\vec{H} = \vec{H}_{eff}$. Following the conclusion of Section 3.2, the magnetic moment will precess about \vec{H}_{eff} in the rotating frame at the frequency $\omega'' = \gamma H_{eff}$.

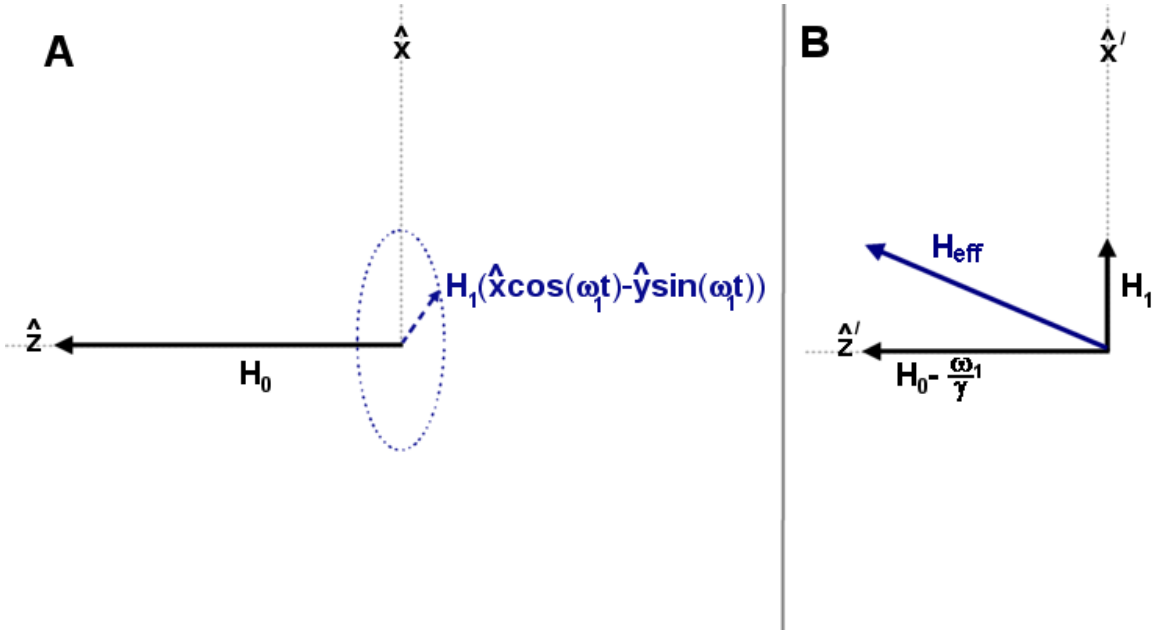


Figure 5: The magnetic fields in the the laboratory frame (A) and the rotating frame (B).

When $|H_1| \ll |H_0|$, \vec{H}_{eff} is nearly aligned with $\pm \hat{z}'$ unless the condition

$$|H_1| \approx \left| H_0 - \frac{\omega_1}{\gamma} \right| \quad (24)$$

is satisfied. In other words, the effect of a field along \hat{x}' is negligible when its angular frequency ω_1 is far from γH_0 . Resonance occurs when

$$\omega_1 = \gamma H_0 \quad (25)$$

during which the effective magnetic field becomes

$$\vec{H}_{\text{eff}} = H_1 \hat{x}' \quad (26)$$

At resonance, therefore, the magnetic moment precesses about \hat{x}' .

3.4 THE CASE OF STATIC AND OSCILLATING FIELDS

During adiabatic fast passage (AFP), the RF coils produce a weak, oscillating

magnetic field $\vec{H}_{RF} = 2H_1 \cos(\omega_l t) \hat{x}$, and the main coils produce a strong, magnetic holding field $\vec{H}_0 = H_0 \hat{z}$ (Fig. 6). The oscillating field can be broken up into two counter-rotating components

$$\vec{H}_{RF} = H_1 [\cos(\omega_l t) \hat{x} - \sin(\omega_l t) \hat{y}] + H_1 [\cos(\omega_l t) \hat{x} + \sin(\omega_l t) \hat{y}] \quad (27)$$

The first component rotates at $-\omega_l \hat{z}$, and the second component rotates at $\omega_l \hat{z}$. Since these fields are much weaker than the holding field $|H_1| \ll |H_0|$, only at resonance can they significantly affect the motion of the magnetic moment.

When the reference frame is chosen to rotate at the frequency $\vec{\omega}_l = -\omega_l \hat{z}$ of the first component, resonance (Eq. 25) occurs at $\omega_l = \gamma H_0$. In this frame, the first component is static along \hat{x}' . The second component, however, is rotating off-resonance at frequency $+2\omega_l \hat{z}'$. Since off resonance rotating magnetic fields do not significantly affect a magnetic moment, the second component of the oscillating field can be ignored in this reference frame.

Neglecting the second component, the effective magnetic field in the frame rotating at $\vec{\omega}_l = -\omega_l \hat{z}$ (Fig. 6) now becomes

$$\vec{H}_{eff} = \left(H_0 - \frac{\omega_l}{\gamma} \right) \hat{z}' + H_1 \hat{x}' \quad (28)$$

Notice Eq. 28 is identical to Eq. 22. The combination of static and oscillating magnetic fields has therefore been reduced to the case described in Section 3.3. The magnetic moment will precess about \vec{H}_{eff} where at resonance, $\vec{H}_{eff} = H_1 \hat{x}'$.

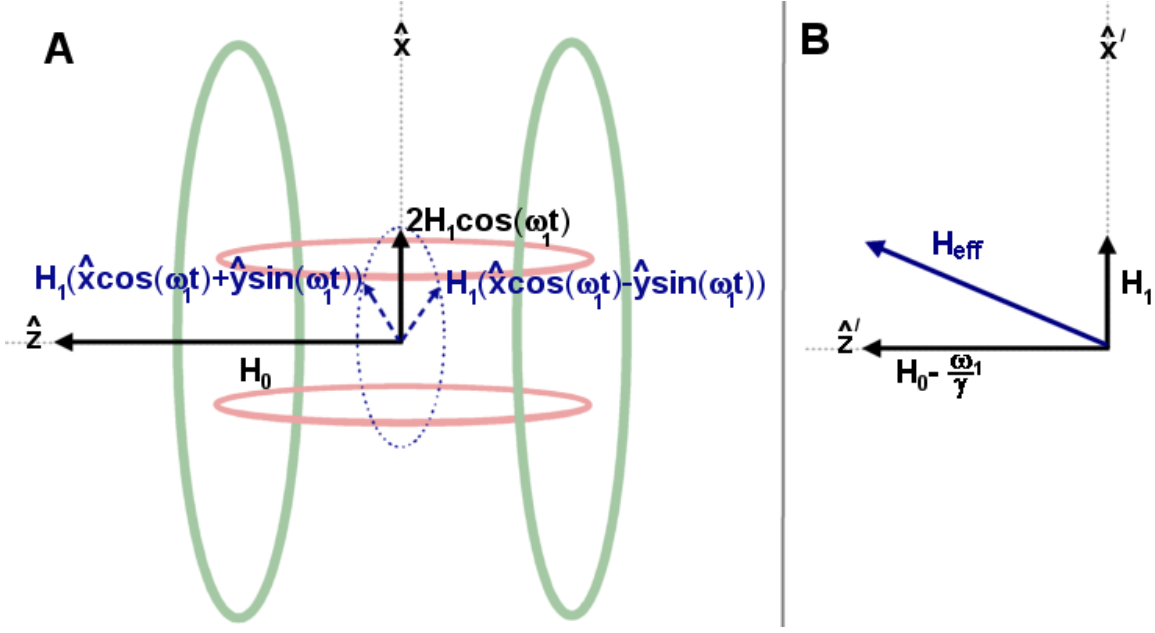


Figure 6: The magnetic fields used in AFP in the coordinate systems of the laboratory frame (A) and the rotating frame (B).

3.5 CONDITIONS OF ADABATIC FAST PASSAGE

During polarization, the ^3He magnetic moments are anti-aligned with the strong, magnetic holding field $H_0 \hat{z}$. For a number density N of ^3He spins with polarization P , the net magnetization is

$$\vec{M} = NP\vec{\mu} \quad (29)$$

Since the ^3He magnetic moment $\mu_{^3\text{He}} = -1.064 \times 10^{-26} \frac{\text{J}}{\text{G}}$ [29] is negative, the net magnetization points in a direction opposite to that of the magnetic moments.

After polarization, a weak RF field $\vec{H}_{RF} = 2H_1 \cos(\omega_l t) \hat{x}$ is applied where $H_1 \ll H_0$. In the frame rotating at $\bar{\omega}_l = -\omega_l \hat{z}$, an effective magnetic field \vec{H}_{eff} is produced (Eq. 28). Initially $H_0 \ll \frac{\omega_l}{\gamma}$ and is below resonance. The effective magnetic

field \vec{H}_{eff} is therefore aligned with the ${}^3\text{He}$ magnetization in the $-\hat{z}'$ direction.

During AFP, \vec{H}_{eff} is rotated about \hat{y}' at a speed slow enough for the ${}^3\text{He}$ magnetization to follow the rotation adiabatically. Since $\hat{z}' = \hat{z}$, an \vec{H}_{eff} rotation from $-\hat{z}'$ to \hat{z}' in the rotating frame will correspond to a reversal in the direction of ${}^3\text{He}$ magnetization and polarization in the laboratory frame. The rotation of \vec{H}_{eff} is achieved by ramping H_0 at constant speed $\frac{dH_0}{dt}$ from below resonance ($H_0 \ll \frac{\omega_1}{\gamma}$) to above resonance ($\frac{\omega_1}{\gamma} \ll H_0$). Typically, the field is then ramped back down to below resonance to restore the initial direction of polarization.

For the spins to follow \vec{H}_{eff} adiabatically, they must precess about \vec{H}_{eff} much faster than \vec{H}_{eff} rotates about \hat{y}' [30]. Since $\frac{dH_0}{dt}$ and H_1 are constant, the maximum rate of \vec{H}_{eff} rotation $\frac{d\theta}{dt}$ about \hat{y}' occurs at resonance where

$$\frac{d\theta}{dt} = \frac{dH_0/dt}{H_{\text{eff}}} \quad (30)$$

and

$$H_{\text{eff}} = H_1 \quad (31)$$

At resonance the spins precess at ω_1 . This sets the adiabatic condition as

$$\frac{dH_0/dt}{H_1} \ll \omega_1 (= \gamma H_1) \quad (32)$$

Relaxation mechanisms dominate during passage through resonance.

Longitudinal and transverse relaxations (with respect to \vec{H}_{eff}) are described by two time constants, T_{1r} and T_{2r} respectively. In the rotating frame, the magnetization is always aligned with \vec{H}_{eff} , and therefore T_{1r} dominates. The time spent near resonance must be short with respect to T_{1r} to maintain polarization and achieve a polarization signal. At resonance $|H_{\text{eff}}|$ is at a minimum, and consequently T_{1r} is shortest. The fast condition

$$\frac{1}{T_{1r}} \ll \frac{dH_0/dt}{H_1} \quad (33)$$

is therefore placed upon the ramping speed $\frac{dH_0}{dt}$ at resonance ($H_{\text{eff}} = H_1$). Combining Eq. 33 and Eq. 32 gives the complete condition for adiabatic fast passage

$$\frac{1}{T_{1r}} \ll \frac{dH_0/dt}{H_1} \ll \gamma H_1 \quad (34)$$

In NMR systems similar to this one, T_{1r} is dependent on the ^3He diffusion constant and magnetic field inhomogeneities[26]. By comparison[18], it is expected that T_{1r} is on the order of 500 seconds. At typical experimental parameters ($H_1 = 80\text{mG}$,

$\frac{dH_0}{dt} = 1.2 \frac{\text{G}}{\text{s}}$) the conditions for adiabatic fast passage are well satisfied:

$$\left(\frac{1}{T_{1r}} = 0.002 \text{ s}^{-1} \right) \ll \left(\frac{dH_0/dt}{H_1} = 15 \text{ s}^{-1} \right) \ll \left(\gamma H_1 = 1630 \text{ s}^{-1} \right) \quad (35)$$

At resonance ($H_0 = \frac{\omega_1}{\gamma}$), \vec{H}_{eff} and the ^3He net magnetization are in the \hat{x}' direction. In the laboratory frame, this is seen as the net magnetization rotating about \hat{z} at the angular frequency ω_l . The magnetization's frequency of rotation ω_l is

equivalent to the oscillation frequency of the RF field. The rotating magnetization \vec{M}_R creates an oscillating magnetic flux within two parallel coils of wire (the pickup coils) near the ${}^3\text{He}$. An emf $\xi \propto \vec{M}_R \propto P$ oscillating at ω_1 is induced in the pickup coils. Using various electronics described in the next section, this voltage (polarization signal) is measured and recorded.

4. EXPERIMENTAL SETUP

Polarization and polarimetry use a variety of electronics, magnets, and optics. In this section, the equipment for optical pumping and NMR will be discussed. Instrument synchronization and computer control will also be noted.

4.1 MAGNETIC COILS AND ELECTRONICS

Efficient polarization and accurate adiabatic fast passage measurements require a very homogeneous holding field. This homogeneity is provided by a pair of large Walker Scientific Inc. Helmholtz Coils (main coils). The coils have a 0.314Ω combined resistance, 500mH inductance, 57 in. inner diameter, 62 in. outer diameter, and 27.25 in. separation (face to face). A KEPCO Bipolar Operational Power Supply powers the main coils in series. The linear relation between the magnetic field magnitude and the current in the coils was determined using a Gauss meter and the power supply display. Since the resistivity of the coils is temperature-dependent, the magnetic field was also measured as a function of time. With -25 V ($\sim 9.0\text{A}$) on the coils, an equilibrium value near -28 Gauss would be achieved after approximately 3 hours (Fig. 7). To ensure temperature stability, the main coils are left on for at least 5 hours before use in a measurement.

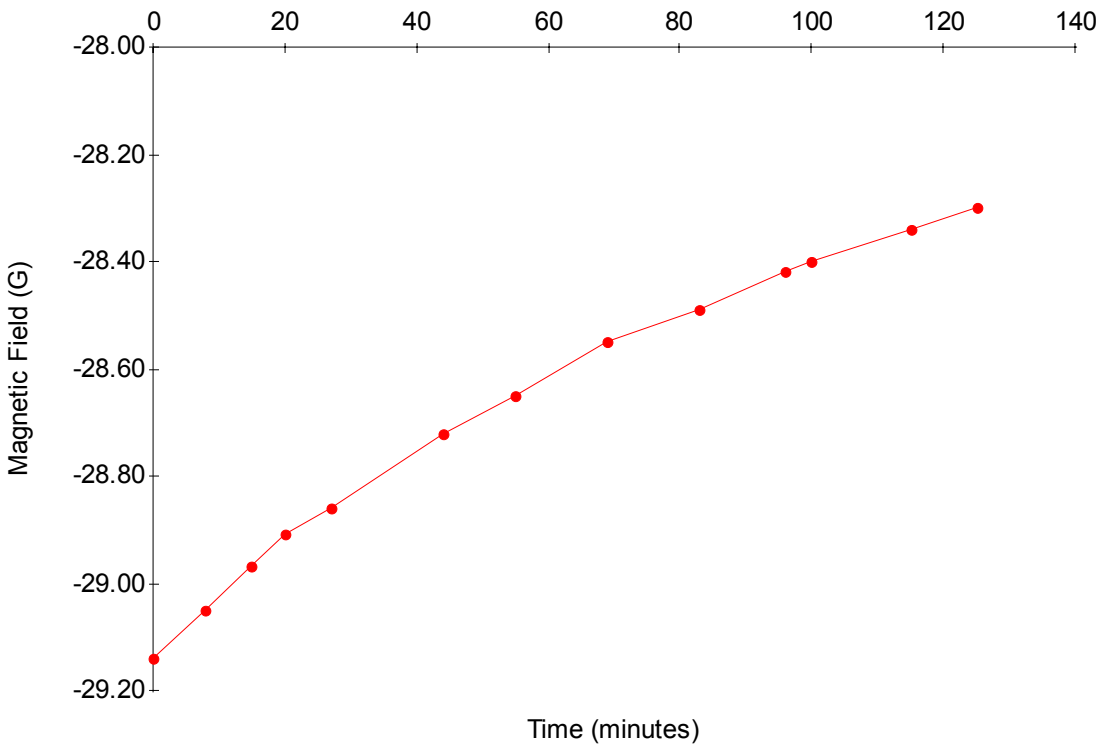


Figure 7: A measurement of the main coils' magnetic field as a function of time with constant input voltage (-25 V). As the coils heat up from room temperature, the magnetic field magnitude decreases as the resistance of the coils increases.

The KEPCO Power Supply is operated in voltage mode and is controlled by an Agilent 33120A Function Generator. This holding field function generator is PC computer controlled via a GPIB interface and LabView software. A DC voltage V_{FG} on the function generator sets a corresponding DC voltage $V_{KEPCO} = 3.59V_{FG} + 0.012V$ at the KEPCO outputs (Fig. 8).

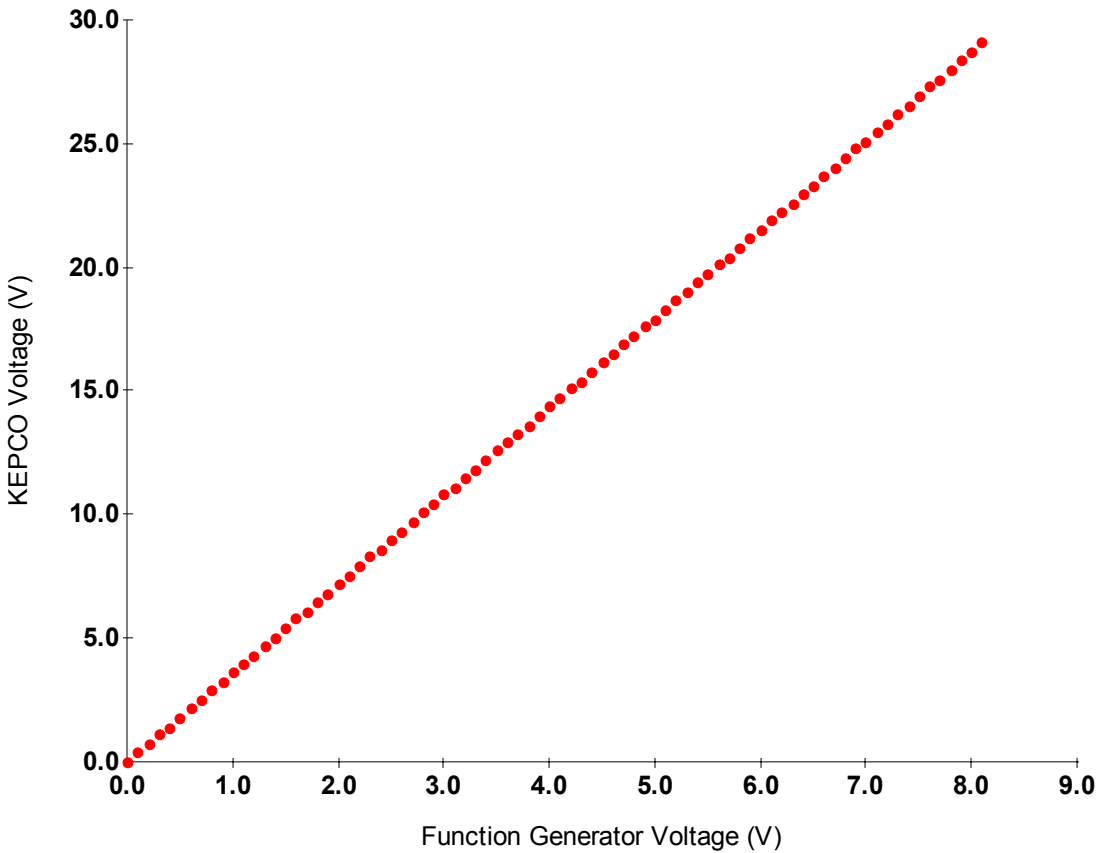


Figure 8: Relation between input voltage V_{FG} and output voltage V_{KEPCO} on the main coils' power supply.

The smaller set of coils, the RF coils, are fixed perpendicular to the main coils and provide the RF field (91 kHz, 80 mG peak-to-peak) used in AFP experiments. The RF coils have $0.7\ \Omega$ resistance, 0.114 mH inductance, 15.75 in. separation (face to face), 33.625 in. outer diameter, and 31.0 in. inner diameter. The relation of current to magnetic field was obtained using a 1.065 in. diameter, 40 turn coil of wire (the H_1 coil). By measuring the induced emf in the H_1 coil placed at the center of the system, the relationship between RF current peak-to-peak I_{RF} and magnetic field peak-to-peak was

established. The magnetic field amplitude H_1 was found to be $H_1 = 26 \frac{\text{mG}}{\text{A}}(I_{RF}) - 7\text{mG}$ (Fig. 9).

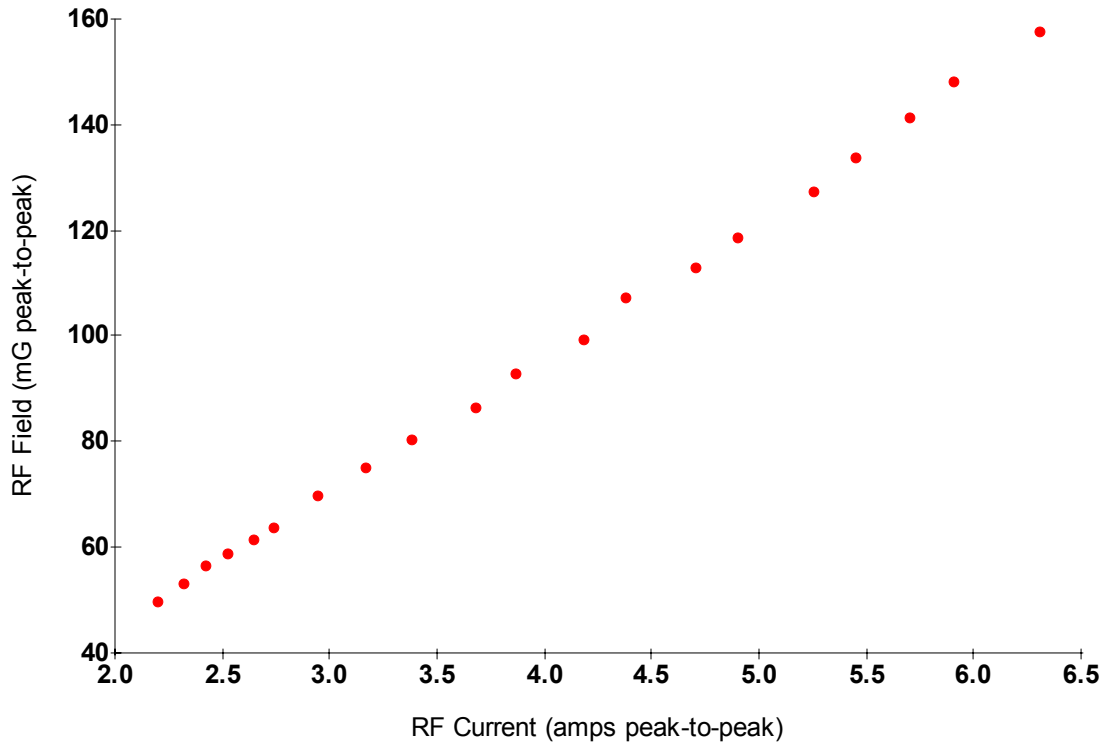


Figure 9: The H_1 calibration relating RF current to RF field amplitude.

A T&C Power Conversion ULTRA 2021 100W Linear Amplifier (53 dB gain) powers the RF coils in series (Fig. 10). A resistance/capacitance box is used in this circuit to reduce reflected power into the RF amplifier (Fig. 11). Reflected power (due to the reactive nature of the load) is potentially damaging to the amplifier in addition to causing heating and instability within the unit. The added capacitance (22nF) counterbalances the inductive impedance of the coils, while the resistive load (10.7Ω) draws current and dissipates power. For an RF field of 80mG peak-to-peak, the power

resistors dissipate about 20W. A vented box is used to allow air-cooling of the power resistors. The RF current monitor is also mounted in this box.

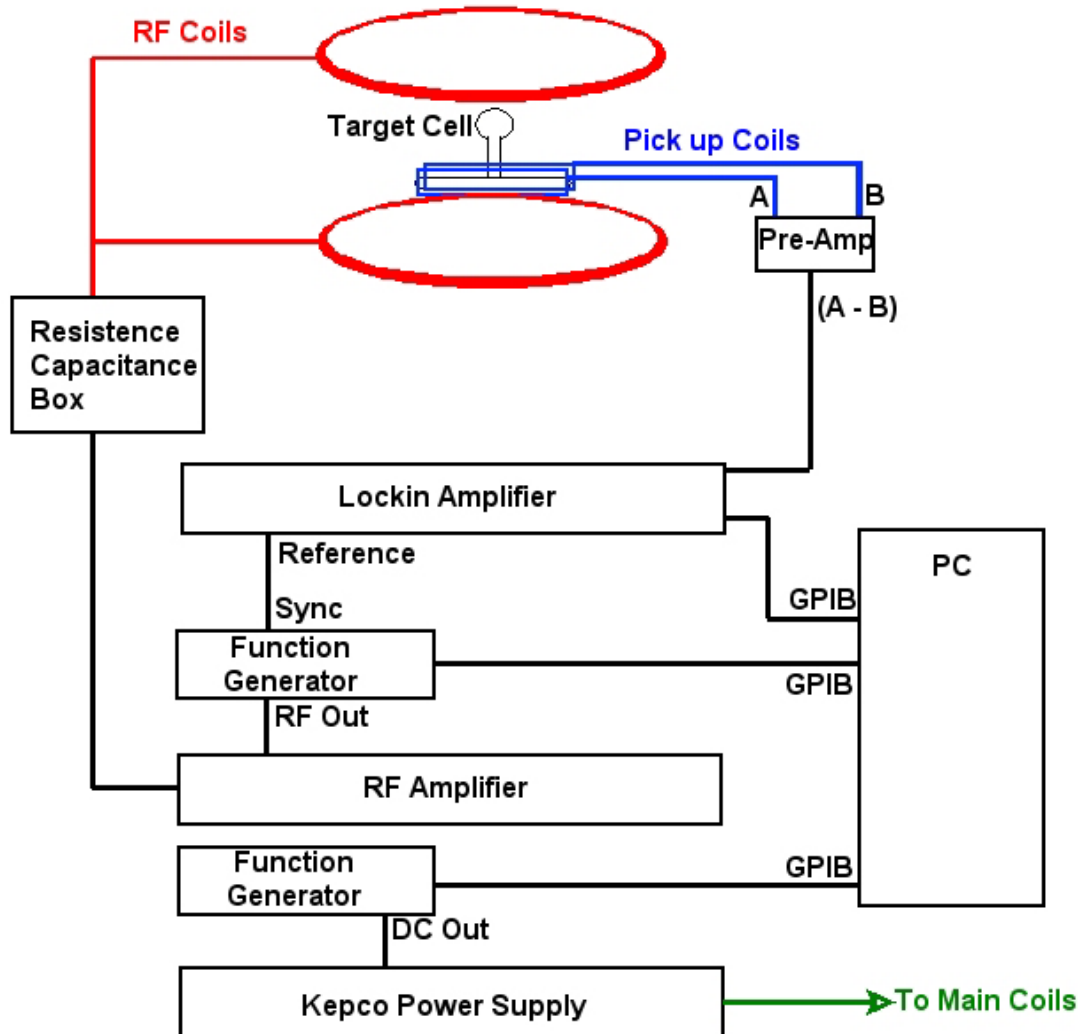


Figure 10: A schematic of the electronics and component connections during typical polarization and NMR polarimetry measurements.

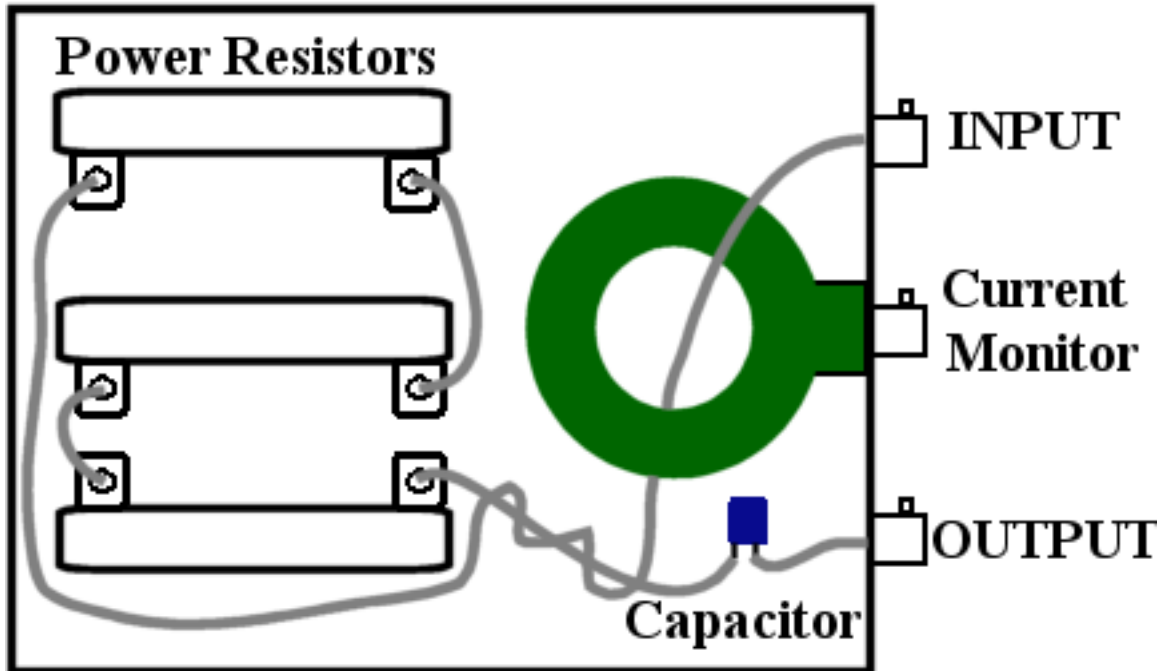


Figure 11: Capacitance/Resistance box with RF current monitor.

A separate Agilent 33120A Function Generator (with GPIB interface and LabView control) controls the RF Amplifier (Fig. 10). Input attenuators (20dB + 3dB) are used to limit and therefore protect the amplifier from excessive amplification. An input voltage of 1.6 V(rms) from the RF function generator corresponds to about 3.3 amps peak-to-peak through the RF coils. The RF field is used primarily during a AFP sweep, and the RF amplifier is sensitive to its internal temperature. This makes it difficult to establish a consistent relationship between input voltage and the RF magnetic field magnitude. Instead, the previously discussed relationship between RF magnetic field and RF current is used.

The third pair of coils, the pickup coils (Fig. 12), is used to detect the 91 kHz AFP polarization signal. These coils are movable to allow precise alignment orthogonal to the other coils. Each pickup coil comprises 100 turns of Belden 8084 36AWG Heavy

Polythermaleze wire wrapped in a 0.16 in. groove around a rectangular area 0.75 in. by 4.33 in. of PVC plastic. Each coil has a 37Ω resistance, a 1.4 mH inductance, and is connected to a breakout box *via* a wire pair that is part of a four conductor cable (Alpha Wire AG 2466C, 2 Pair, 22AWG, Shielded 75C). This breakout box enables standard BNC cable connections to each pickup coil. The outputs for Coil 1 and Coil 2 are respectively connected (Fig. 10) to the A and B channels of a Stanford Research Systems SR560 Preamplifier. The preamplifier output is the differential of these two channels (A - B) and uses a 6dB 10kHz high-pass filter and 6dB 100kHz low-pass filter to aid in isolating the 91kHz AFP polarization signal. The preamplifier also has incremental gain settings that are used during coil alignment.

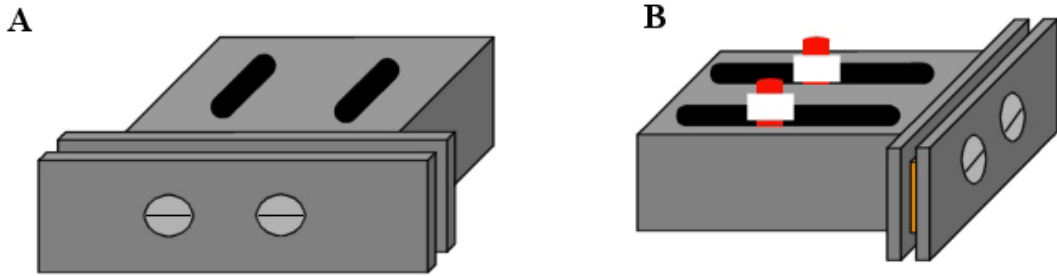


Figure 12: Perspective views of a pickup coil. Two screws secure the faceplate that establishes the groove for the wire windings. Two long slots allow the pickup coil to move along bolts (B) and be precisely aligned.

A Perkin-Elmer 7265 Lock-in Amplifier is connected to the output of the preamplifier. The lock-in amplifier is used to measure the preamp output voltage at a very specific frequency determined by the reference channel. Typically the lock-in amplifier is referenced with the sync signal of the RF function generator (91kHz square

wave). The lock-in amplifier is also GPIB interfaced for computer control and data recovery.

4.2 TARGET CELL AND OVEN

Target cells used in this work are constructed with hand blown aluminosilicate glass (General Electric type 180). The two-chamber design (Fig. 1) allows ^3He polarization in the upper (pumping) chamber and electron- ^3He scattering in the lower chamber. The upper chamber is a 2.5 in. diameter sphere. The cylindrical transfer tube is 2.5 in. long with a 0.5 in. diameter. The lower chamber is 40 cm long with a 0.75 in. diameter. All walls of the target cell excluding the end windows were made about 1mm thick. The end windows are about 140 microns thick to minimize glass interactions with the electron beam during a scattering experiment at Jefferson Lab.

A detailed description of cell filling is given in Ref. [17]. Briefly, the cell is first connected to a high vacuum system ($\sim 10^{-8}$ torr) and baked (470° C) to remove any impurities prior to filling. A small amount of Rb is then added to the pumping chamber. Finally, the cell is filled to a pressure of 60 torr (at room temperature) of N_2 , 8.5 amagats of ^3He , and sealed.

When the cell is ready for the polarization procedure, it is positioned in the NMR system at the center of the three sets of coils. It is mounted with high temperature silicone rubber adhesive sealant (General Electric RTV 106) to a suspended Teflon oven that encloses the pumping chamber of the cell.

The oven measures 4.25 in. wide, 4.25 in. long, and 5.125 in. high with 1/2 in. and 3/8 in. thick Teflon walls. Two 3 in. diameter glass windows in the oven allow the

laser light to enter, pass through the pumping chamber, and exit to the laser dump. To vaporize the Rb needed for optical pumping, the oven heats to 170°C using a forced hot air system. A resistance temperature detector (RTD) within the oven reads out the temperature to an oven controller operating two inline 750W heaters. This design allows remote placement of the heaters and minimizes the amount of metal within the coils. Conductors near the system cause depolarizing magnetic field gradients and introduce noise in the NMR system. Non-metallic bolts, PVC and Teflon construction materials, and an emf shielded room are other design features of the lab intended to reduce gradients.

4.3 LASER AND OPTICS

A diode laser (Coherent FAP 30W Diode Laser) and a system of optics are used to supply the positive helicity, circularly polarized, 795nm photons needed for optical pumping of Rb. An optics schematic is given in Fig. 13. Light from the laser (795nm) is directed into the optics system by the use of an optical fiber. The first lens (focal lens) provides a beam size of diameter approximately 2.5 in. at the target cell. The polarizing beam splitter cube separates the light into two equally intense, linearly polarized beams. The beam that passes straight through the cube is vertically polarized. This beam reflects off of a mirror, passes through a single quarter-wave plate, and is sent toward the target. The other beam, which is initially reflected by the cube, is horizontally polarized. This beam passes through a quarter-wave plate, reflects from a mirror, and passes through the same quarter-wave plate, the cube, and a final quarter-wave plate on its way to the target. In this optical path, the first two quarter-wave plate passes are used as an effective half-

wave plate to rotate the linear polarization 90 degrees to give vertical polarization. This process is needed to pass back through the polarizing beam splitter without losing intensity. The final quarter-wave plate in both beam paths circularly polarizes the photons.

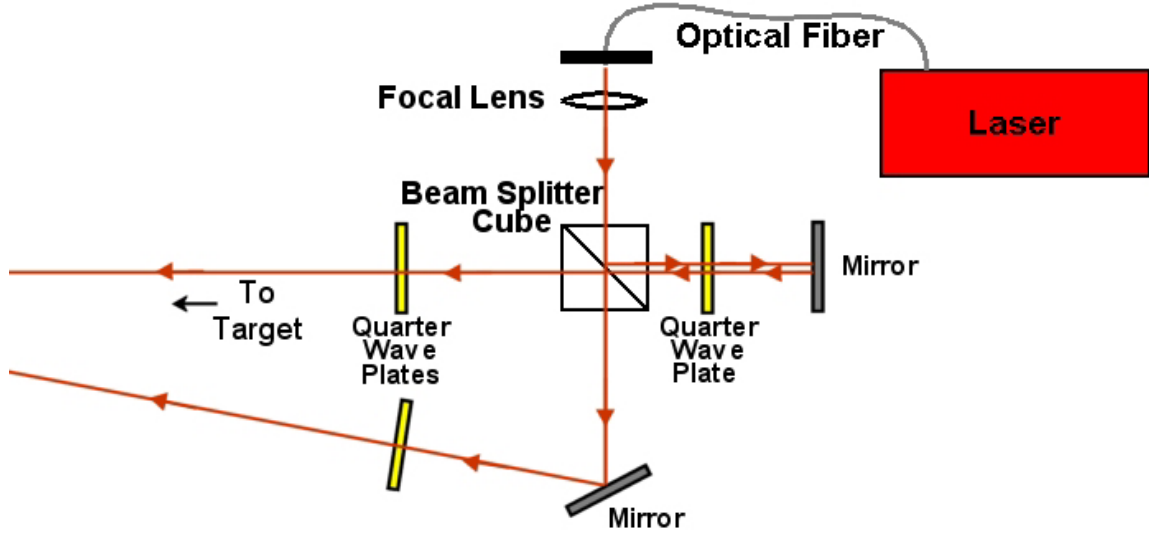


Figure 13: A schematic of the optics used to generate circularly polarized, 795nm photons and project them onto the pumping chamber of the target cell.

Quarter-wave plates are designed with two perpendicular axes (Fig. 14). To obtain circularly polarized light, linearly polarized light is aligned directly between these two axes. The component of the light whose polarization is projected along the slow axis is retarded 1/4 of a wavelength (90° phase difference) as compared to the component whose polarization is projected along the fast axis. When these phase-shifted components are recombined, they produce a resultant polarization of fixed magnitude that rotates in the plane of the wave plate. This is defined as circularly polarized light.

Positive helicity $+\sigma$ is obtained when the resultant polarization rotates clockwise, looking in the direction of propagation. This condition is met when the fast axis, the slow axis, and the direction of light propagation form a right-handed set. If two quarter-wave plates are used in series, a $1/2$ -wavelength delay (180° phase difference) is introduced which rotates the linear polarization 90° .

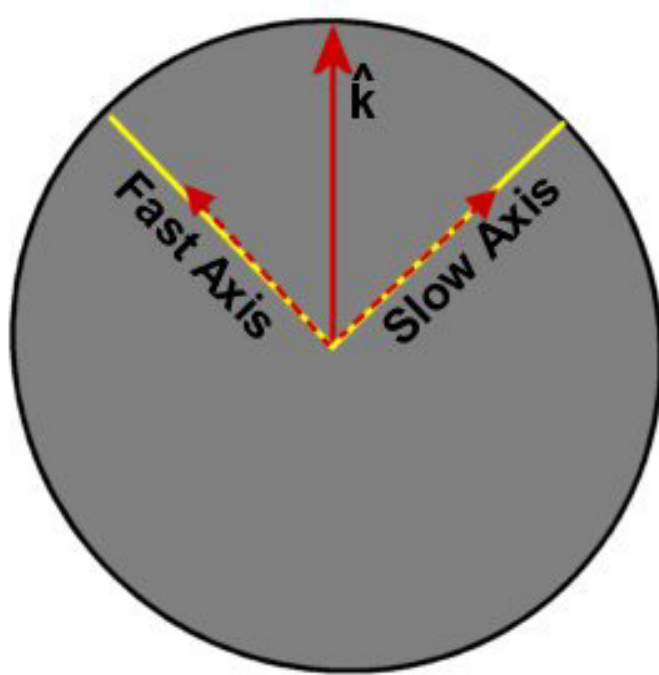


Figure 14: A quarter-wave plate positioned to produce $+\sigma$ photons. Incident light is propagating into the page with linear polarization \hat{k} . The components of the polarization vector along the fast and slow axes are shown with dotted lines.

5. EXPERIMENTAL PROCEDURES

5.1 PICK-UP COIL ALIGNMENT

During AFP, the rotating magnetization of the ^3He spins induces an emf in the pickup coils on the order of a few mV(rms). This signal is at the same frequency of the

RF magnetic field (91 kHz). If the pickup coils are not exactly aligned orthogonally to the RF field, signals from the RF coils (seen as noise) will prevent measurement of the polarization signal.

Once a target cell has been mounted in the oven, the pickup coils can be aligned. To achieve a large polarization signal, the coils are positioned within a few millimeters of the cell. During oven heating, the cell may move slightly. Enough space is therefore left between the cell and the pickup coils to ensure that pickup coil alignment is maintained and that the high-pressure cell does not rupture. During alignment, the RF Field (91kHz, 80mG peak-to-peak) is turned on, and an oscilloscope monitors the pickup coil response, which has been passed through the preamp (Gain = 2, 10k high-pass frequency filter, 100k low-pass frequency filter). The pickup coils' positions are then tilted and positioned using plastic shims (sizes from 0.03 in. to 0.004 in.) to reduce the noise amplitude. For efficient coil alignment, the signal from each preamp channel (A, B) is analyzed separately first. Then the differential signal (A-B) is optimized. Good positioning of the coils results in 91 kHz noise of a few μ V(rms) or less. Initially, this procedure was performed while the oven was turned off. It was discovered, however, that the noise in the coils has a dependence on the temperature in the oven (Fig 15). Since polarimetry is done with the Rb vaporized, future coil alignments will be conducted with the oven on.

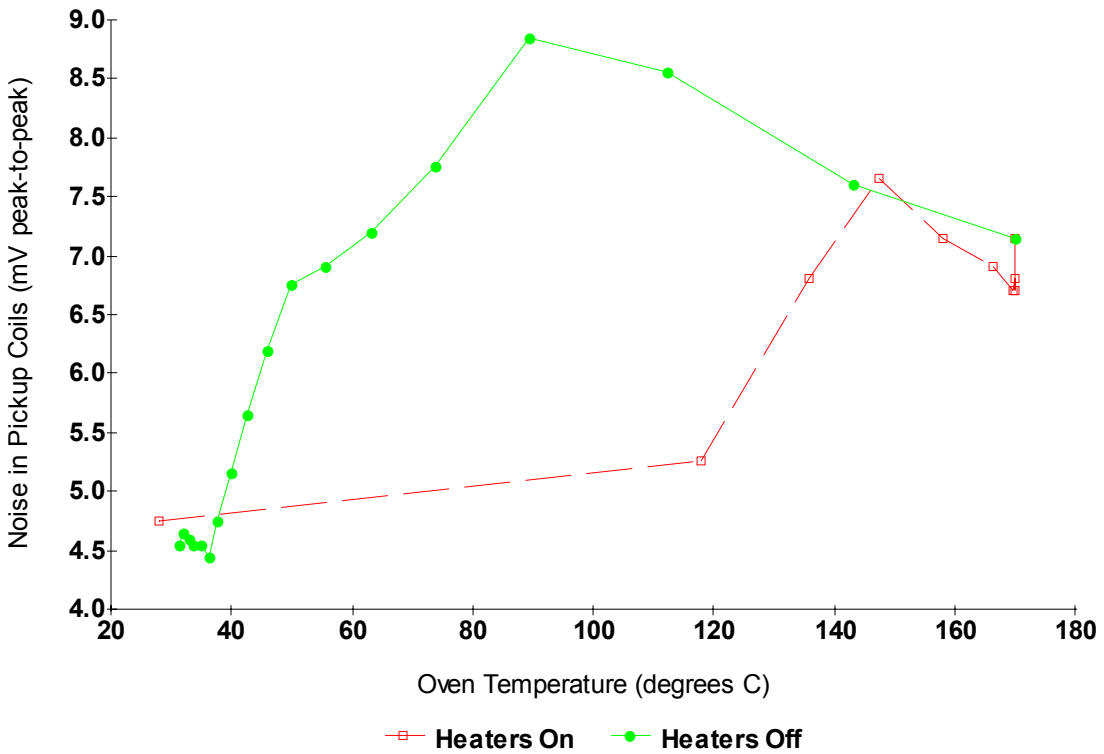


Figure 15: The dependence of pickup coil noise on oven temperature.

5.2 Q-FACTOR OF THE PICKUP COIL CIRCUIT

The Q-factor of the pickup coil circuit is needed to adjust polarization data from multiple experiments. To measure this, 200 turns of Belden 8081 30 Gauge Heavy Polythermaleze wire were wrapped around a 1.25 in. diameter spool and aligned parallel to the pickup coils. This coil (Q-Coil) is used to create an oscillating magnetic field that is detectable by the pickup coils. During a Q-curve measurement, the RF Function Generator (3.5V(rms)) directly powers the Q-Coil. A LabView program (“NMR Q Curve WM.vi”, Appendix A.1) is used to ramp the frequency of the RF Function Generator from 60 kHz to 250 kHz in steps of 0.5 kHz. At each step, the pickup coil

response is measured 50 times with the lock-in amplifier and averaged (Fig. 16). The gain of the Q-Coil across this frequency range is nearly constant.

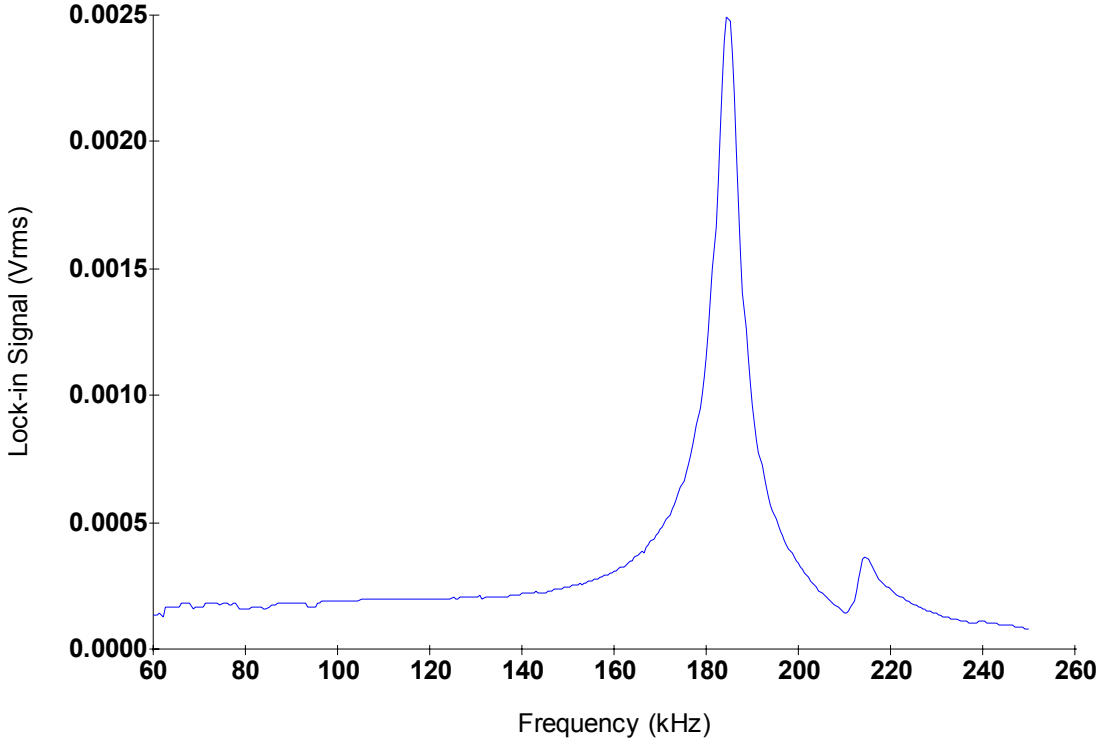


Figure 16: Q-curve measurement of pickup coil circuit. The resonance (185 kHz) was designed to be away from 91 kHz for stability. The cause for the peak at 215 kHz is unknown, but the peak is stable and does not affect the circuit at 91 kHz where polarimetry measurements are made.

5.3 LASER TUNING

The atomic transition used in optical pumping requires 795 nm wavelength photons. To ensure that the laser produces these, a spectrum analyzer (Ocean Optics USB2000 Spectrum Analyzer) is used to characterize the laser output. Fig. 17 shows the laser profile after absorption by the Rb vapor. The width of the absorption line is

possibly due to Doppler shifts and glass refraction. Tuning of the laser involves adjusting the diode laser temperature to move the laser peak to the Rb absorption line.

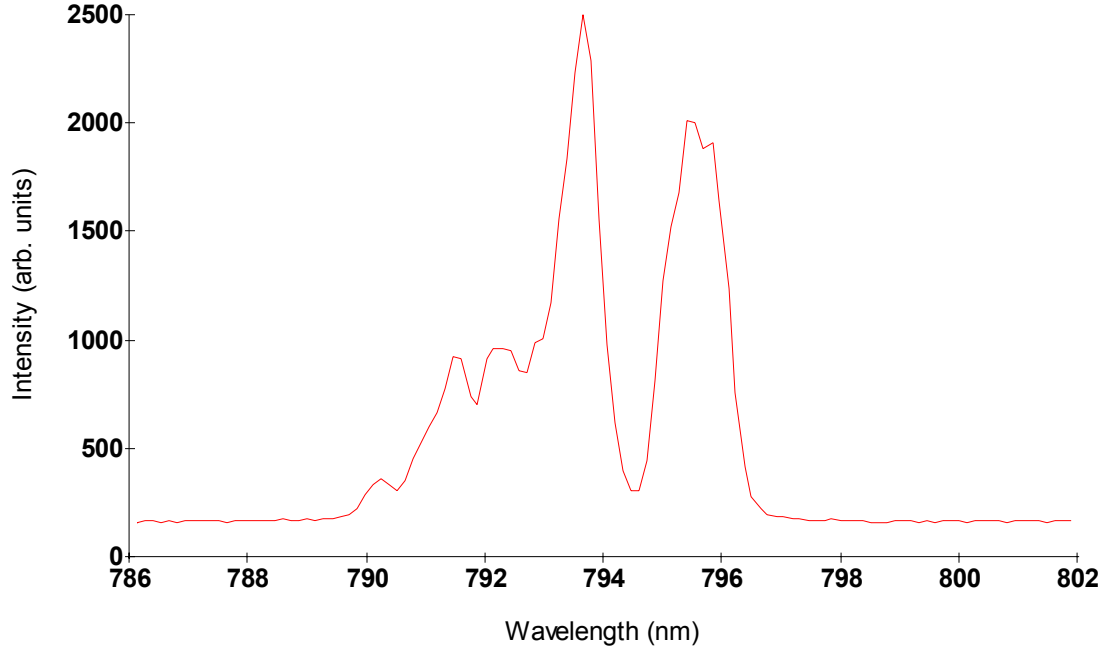


Figure 17: The laser spectrum after passing through Rb vapor in the pumping chamber. Although the wavelength shown here has not been thoroughly calibrated, the absorption line (794.5 nm) lies within the laser centroid (793 nm – 796.5 nm).

5.4 POLARIZATION

To polarize ^3He , the target cell is first mounted in the Teflon oven. Preliminary pickup coil alignment is then performed and, if needed, a Q-curve measurement is taken. The oven is then heated to 170°C and a final pickup coil alignment is made. The program “NMR Load Sweep.vi” (Appendix A.2) is now run. This sets the holding field in the main coils (typically 25 G) and prepares the holding field function generator for AFP.

The RF function generator should be set at an output of 0V DC level. The laser is now turned on, and the cell begins to polarize. The time to reach maximum ^3He polarization is dependent on the target polarization lifetime. For a good target cell, this is on the order of two days. Detectable polarization is achieved, however, after a few minutes.

5.5 POLARIMETRY

The polarimetry measurement is computer controlled by the program “NMR Helium XY FG-V WM.vi” (Appendix A.3). The preamp must be set beforehand to: Gain = 1, 10k high-pass filter, 100k low-pass filter, low noise output, and differential (A-B). The software initializes and configures the function generators and lock-in amplifier. The RF function generator then applies a sinusoidal voltage to the RF amplifier, which produces the RF field (91kHz, 80mG peak-to-peak). A trigger signal is then sent by GPIB to the holding field function generator to begin the main field sweep. This sweep typically ramps the holding field from 25 G to 32 G and back to 25 G at a speed of 1.2 G/s. During both ramp up and ramp down, resonance (about 28 G) is passed through.

The lock-in amplifier is synchronized to a trigger signal from the SYNC channel on the holding field function generator and is referenced to the RF function generator. When the holding field function generator begins its main field sweep, the lock-in amplifier is triggered and begins taking voltage measurements of the preamp output (A-B) 100 times a second. The data from both ramp up and ramp down are stored in the lock-in amplifier’s internal curve buffer. After the ramps are completed, the data are

downloaded via GPIB to the computer. Voltage peaks correspond to the emf induced at resonance (Fig.18).

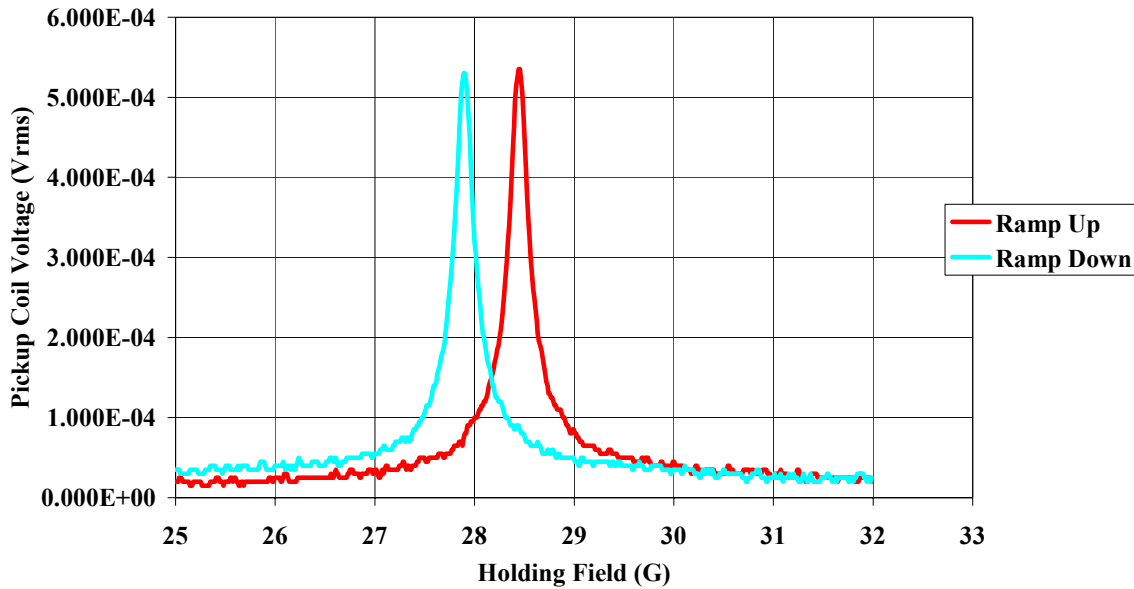


Figure 18: An AFP polarization signal. Resonance occurs at the voltage peaks. The difference in the resonant holding fields is possibly due to imperfect synchronization between instruments.

6. CONCLUSIONS AND FUTURE RESEARCH

Presently, only relative polarizations can be measured with this NMR system. For absolute polarimetry, calibration using de-ionized water is needed. The protons in the hydrogen atoms of water achieve a thermal equilibrium polarization that is calculable and is measurable using AFP. The polarization signal, however, is many orders of magnitude smaller than the ^3He signal and is therefore difficult to detect.

The characteristics of the NMR system also need study. During AFP, some polarization is lost due to relaxation mechanisms. These losses need to be understood in

order to compare multiple polarimetry experiments. The time constant T_{lr} is related to magnetic field gradients and inhomogeneities. It can be studied by varying the magnitude of H_1 . Comparison of polarimetry results with other target labs is possible to evaluate aspects of lab design.

In support of experiments at Jefferson Lab, ^3He target cells can now be characterized using this lab. The lifetime of ^3He target polarization, the rate of polarization, and the maximum polarization can be measured. This lab allows the characteristics of cell design, construction, and filling procedures to be examined and improved. In addition, this lab offers the opportunity for studies unrelated to ^3He target polarization. Polarization of other noble gases is possible with the optical pumping equipment, and the NMR system can be adapted to new research.

The polarization of ^3He and the detection of that polarization attained the principle goals set forth by this honors research. Construction of this lab began with an empty room where a functional NMR and optical pumping system now exists. These accomplishments allow future endeavors to improve ^3He targets and study the mechanisms of polarization and NMR.

APPENDIX A – SOFTWARE DOCUMENTATION

A.1 “NMR Q Curve WM.vi”

PURPOSE:

To measure the response (Q-factor) of the pick-up coils over the range of 60 kHz – 250 kHz using a small loop of wire.

The small loop of wire, the Q-Coil, is connected to the RF Function Generator (Right Agilent 33120A, GPIB address 11) directly and is aligned parallel with the pick-up coils. The pick-up coils are connected to the lock-in amplifier (Perkin-Elmer 7265, GPIB address 12) via preamp. This VI will ramp the frequency of the function generator from 60kHz to 250kHz in steps of 0.5kHz at an amplitude of 3.5 Vrms. At each step, the lock-in takes 50 measurements of the voltage at 10 millisecond intervals. Between each step is a 2 second pause. This data is then presented on screen and then optionally saved as “c:\NMR Data\Q Curve\q_curve <time&date>.dat”

SUB VIs REQUIRED:

“Initialize PE Lockin.vi”

“Read PE Lockin.vi”

“NMR Save Single.vi”

“GPIB readwrite.vi”

FRONT PANEL:

This version has the title “Q Curve Pick-up Coils” written in black on a yellow background.

The upper right has controls to start (“GO”) and to quit (“EXIT”) to be used after starting the program (Ctr-R as with any LabView program).

Beneath these are indicators (Stage, Frequency, Minutes Remaining, Filename) and controls. The controls should be initialized as followed and should not need adjusting:

RF FG Vrms (V) = 3.500

Time to wait....(ms) = 10

Save? = YES!

The plot shows lock-in Vrms on the Y-axis and frequency along the X-axis.

The filename used to save is displayed at the bottom.

DIAGRAM:

Frame	Description
Outside	Here are controls for the “GO” and “EXIT” buttons.
True	
0	A statement regarding operating conditions. Initializing stage is

- indicated. Indicators blanked or set to zero.
 1 Date and time are recorded.
 2 Function generator is turned off. (DC shape with zero offset)
 3
- 0 Lock-in is initialized using the subVI “Initialize PE Lockin.vi”.
This gives a standard operating mode.
 - 1 Pause for command activation.
 - 2 The display on the lock-in display is now configured for Q-Curve measurement. The sensitivity is set to 10mV.
 - 3 Pause for command activation.
- 4
- 0-2 Function Generator is setup to SIN wave at 3.5 Vrms. The frequency selected is 60kHz.
- 5 Pause for command activation.
 6
- FOR This FOR loop will run once for each step in the frequency sweep ((250kHz - 60kHz)/0.5kHz = 380 steps)
 - 0 The current frequency is calculated, sent to the RF Function Generator, and displayed on the front panel. This frequency is also sent outside the loop to be gathered into an array (the X-axis values).
 - 1 A rough calculation of the time remaining is indicated for the user.
 - 2 Pause for lock-in to settle on new frequency
 - 3 Get average measurement using “Read PE Lockin.vi”. The output of this subvi is the average Vrms. This value is sent outside the loop to be gathered into an array (the Y-axis values).
- 7 RF Function generator is “turned off”.
- 0 Voltage is minimized
 - 1 Frequency returned to 91kHz
 - 2 Shape set to DC, no offset.
- 8 Lock-in is returned to a standard operating level.
 9 Plot is created from the two arrays.
 10 Data is saved using “NMR Save Single.vi”. Saving stage is indicated.
 11 Completed stage indicated.
 12 Instructions to return cables to normal positions.

A.2 “NMR Load Sweep.vi”

PURPOSE:

To setup the holding field function generator (Agilent 33120A, GPIB 10) for an NMR sweep.

Before an NMR measurement is taken, this VI should be run. It loads the indicated sweep waveform for the holding field function generator (for the main coils) and configures that function generator’s settings (output termination, burst mode, function shape, voltage units, amplitude, frequency, offset, trigger source, number of bursts). After running the VI (which may take a few minutes), the function generator will be armed and ready for a trigger from the computer (supplied by an NMR measurement VI) to playback the waveform.

When the waveform is played, the SYNC signal of the function generator will drop from HIGH to LOW.

SUB VIs REQUIRED:

“AGILENT LOAD WAVEFORM.vi” (Appendix A.4)

“GPIB readwrite.vi”

“GPIB Error Report.vi”

FRONT PANEL:

This version has the title “NMR Load Sweep” written in black on a white background. Controls are shown as values with a colored background (cyan, orange, green). Indicators have a gray background.

The top left indicators will report errors in commands previously sent to the function generator. If this happens due to a “settings conflict” (ex. the offset was too high), it is likely that commands were run out of order. To correct this, run the program again with the same settings.

The top right control is the address that will receive the commands.

Below these is the main box. The left buttons indicate whether or not to send each command to the function generator. The numbers beside them indicate the order in which the commands are sent. All calculations are always made regardless and displayed on the indicators.

The upper part of the main box contains the controls for the waveform.

Default Control Values:

Waveform Points	15999
Sit time (sec)	0.000 (For 3He measurement not H ₂ O calibration)
Inputs	Magnetic Field
Max Field (G)	32

Min Field (G)	25
Gauss/sec	1.2
alpha calibration data)	3.9539 (This value should be entered from Main Coil
beta calibration data)	0.1507 (This value should be entered from Main Coil
Output Termination	High
Burst Mode	ON
# of burst cycles	1
Select Waveform	VOLATILE

NORMAL OPERATION:

Before running this VI, select the input to be “Magnetic Field” (orange). Enter the parameters in the orange boxes. Alpha and beta should come from main coil calibration data since these values depend on the resistance (and therefore the temperature) of the main coils. Activate all commands *except* the trigger. Finally run the program. If all 15999 points are used, this may take up to 1.5 minutes.

OTHER OPERATIONS:

This VI may also be used as a quick way to adjust the function generator by selecting individual commands. For instance, a loaded waveform may be examined using a scope and by sending the trigger command. Also the Max/Min/Slope values of the waveform can be specified using output voltage instead of magnetic field values by switching the INPUTS switch.

The Select Waveform Control can be used to output any waveform the function generator knows. Enter SIN, SQU, TRI, RAMP, NOIS, or USER or select an arbitrary waveform to be assigned into the USER slot by entering its name. Note: (a list of available arbitrary waveforms can be generated by running the AGLIENT STATUS.VI)

DIAGRAM:

Frame	Description
0	Conversion from Magnetic Field values to Voltage values.
1	Amplitude, Period calculated.

(The following commands make use of the subvi “GPIB readwrite” to communicate to the instrument)

0	Check Standard Event Register
1	Check for Errors
2	Set Output Termination
3	Set Burst Mode
4	Change the FG output to the User defined waveform
5	Change the User defined waveform to the “NMR_WAVE”
6	Load Waveform
0	Indicate Download Status - WORKING

waveform (Note: A waveform by this name must exist. To create one, send the command “DATA:COPY NMR_WAVE, VOLATILE”)

1 Run “AGLIENT LOAD WAVEFORM.VI” subvi. This calculates and sends the waveform to the FG.

2 Indicate Download Status - DONE

- 7 Set Voltage Units
- 8 Set Amplitude
- 9 Set Offset
- 10 Set Frequency
- 11 Set Number of cycles per burst (i.e. per trigger)
- 12 Set the trigger source to the computer bus
- 13 Either sets the selected arbitrary waveform to the USER waveform, or sets the output waveform to the selected shape (SIN, DC, USER, TRI, SQU, RAMP, NOIS)
- 14 Sends a single trigger to the Function Generator.

A.3 “NMR Helium XY FG-V WM.vi”

PURPOSE:

This VI is the main program for performing an NMR Sweep and recording the induced voltage in the pickup coils.

This VI communicates with the RF function generator (Right Agilent 33120A, GPIB address 11), holding field function generator (Left Agilent 33120A, GPIB address 10), and the lock-in amplifier (Perkin-Elmer 7265, GPIB address 12).

After initializing the system, a trigger is sent to the holding field function generator (to begin the main field sweep) which is SYNC'd to the lock-in. This SYNC signals the lock-in to start taking data at 100Hz. This data is stored in the lock-in curve buffer and is retrieved by this VI after the sweep. This data is finally plotted and saved to a file in “C:\NMR Data\3He\”.

SUB VIs REQUIRED:

“NMR Save Single.vi”

FRONT PANEL:

This version has the title “NMR Measurement” in white letters on an orange background.

The upper left indicators, show the start and stop time of the measurement.

The plots below will show the lock-in amplifier values of the pickup coil voltage as a function of the magnitude of the holding field.

At the upper right, the stage is indicated. Above this is an RF status indicator. Beneath this is a start button and a light. The light indicates the program is running.

The indicators beneath these give the date and time the measurement was run. The teal colored boxes are controls for the plots. The two displays “X Download” and “Y Download” show the progress of retrieving each channel from the lock-in curve buffer.

An RF Voltage control, Lock-in Sensitivity control, Number of sweeps control, and Minutes between Sweeps are present. The lock-in phase and Current Sweep Number are indicated.

Other indicators and controls lie off screen to the lower left, and are not used in normal operation.

NORMAL OPERATION:

Before running this VI, the holding field function generator should be armed and awaiting a trigger signal. This is accomplished with the “NMR Sweep.vi” program.

A polarized target cell should be in place. The KEPCO Power Supply should be connected to the main coils and controlled by the holding field function generator. The

RF Amplifier should be connected to the RF Coils through the Resistance/Capacitance Box and controlled by the RF function generator. A scope can be used to monitor the current in the RF Coils using the R/C Box's current meter. The lock-in amplifier should be connected to the preamp and referenced to the RF function generator. The preamp should be connected to the pickup coils through the breakout box.

Preamp settings:

- Gain =1
- Gain Mode = Low Noise
- Filters = 10k, 100k
- Rolloff = 6dB/oct
- AC Coupling
- Mode = A-B

The voltage for the RF function generator should be set on the front panel for a field of about 80 mG (this can be adjusted for gradient studies). For our system, that corresponds to about 3.3 Amps (measured peak to peak) of current through the RF coils. The Lock-in Sensitivity should be adjusted (typically about 50mV) but an auto-sensitivity command will override this control. The number of measurements is controlled by "Number of sweeps". The time between sweeps should also be selected

After starting the program, click the GO button. Follow the dialog boxes.

DIAGRAM:

	Description
Frame	
Outside	The large box is actually a while loop. The green light is reset to off.
rest	The large "GO" button controls the T/F control which starts the of the program.
False	
True	Initializations :
0	Start Stage is indicated. Graphs are cleared, certain variables zeroed.
1	Setup RF Function Generator
0	Green light on. Query user if Holding Field FG is ready
True	
False	Green light off, Stop running.
1	Make sure RF FG is off (DC level. 0V). Initialization Stage. Make sure RF indicator light is off.
2	Set RF FG units to Vrms
2	
0	Initialize Lock-in. Set display to X volt, Mag, Phase, Y voltage.
1	Pause for command activation

2 Set reference mode, input mode
 3 Pause for command activation
 4 Set sensitivity according to control
 5 Pause for command activation
 3
 0 Prompt to turn RF on, else stop program
 1 RF ON Stage
 2 RF FG is set to output SIN wave at 91 kHz, Specified Voltage (1.5 Vrms default), and 0 Offset. RF light is on.
 3 Prompt to write down RF Current
 4
 0 Lock-in is setup. User is asked if Autophase is wanted.
 True AutoPhase command sent, pauses for activation
 1 User is asked if AutoOffset is wanted
 True AutoOffset command sent, pauses for activation
 2 User is asked if AutoSensitivity is wanted
 True AutoSensitivity command sent, pauses for activation, prompts user to see if sensitivity is set
 5
 0 Phase is requested from Lock-in
 1 Phase is read from Lock-in
 2 Phase is displayed
 6 (upper left) Start Time is indicated.
 7
 Number of points spent at top of waveform (used in H2O calibration), Sit Points, is calculated.
 Waveform variables are declared (speed=slope) “Speed (G/s), Bmax (G), Bmin (G)” for main holding field.
 The change in magnetic field, “delta B”, is calculated.
 The “Ramp up time” is calculated.
 For Loop
 0 Used in multiple sweep applications.
 1 Get time and date of this sweep.
 1
 0 Calculate how many Curve Buffer Points we will need. Setup lock-in curve buffer to store X, Y, and Sensitivity at 100 Hz when given an external trigger (from FG SYNC).
 1 Wait for command activation.
 2 Ramping Stage. Send Trigger to Holding Field FG to play ramp waveform. The sync signal (that is inverted) from the FG will trigger the lock-in to record.
 3 Wait for ramp up and ramp down (add an extra second for command activations)

- 4 RF OFF Stage. RF light off. RF FG turned “off” (DC level.)
 5 READING X Stage. Dump X Channel to Computer
 6 X Values are recovered from Lock-in
 While LOOP Repeats until done (status bit 1 asserted)
 An indication of progress is done in the lower left.
 0 A value is read from the lock-in and converted to a number.
 1
 While LOOP
 Keeps checking the status register to see if another piece of
 data is ready (status 7) or is done (status 1).
 7 READING Y Stage. Dump Y Channel to Computer
 8 Y Values are recovered from Lock-in
 While LOOP Repeats until done (status bit 1 asserted)
 An indication of progress is done in the lower left.
 0 A value is read from the lock-in and converted to a number.
 1
 While LOOP
 Keeps checking the status register to see if another piece of
 data is ready (status 7) or is done (status 1).
 9 B-Field Values are calculated based on waveform parameters.
 10 X Channel Data is graphed with B-Field values and saved to
 “C:\NMR Data\3He”
 11 X Channel Data is graphed with B-Field values and saved to
 “C:\NMR Data\3He”
 2 Latest NMR measurement file is deleted.
 3 Latest NMR measurement file is saved with latest X Channel
 filename.
 4 Checks to see if another sweep is needed. If so, download
 indicators are cleared and system waits according to front panel control.
 8 Stop Time is indicated.
 9 COMPLETED Stage. Green light turned off
 10 Program Stop.

A.4 “AGLIENT LOAD WAVEFORM.vi”

PURPOSE:

A subvi for “NMR Load Sweep.vi” to calculate and send the holding field waveform. This waveform is a ramp up to a plateau where it sits and then ramps down. Each point is given a value between 0 and 1.

INPUTS/CONTROLS:

Period, sit time, whether to send to FG, number of waveform points to use, GPIB address

OUTPUTS/INDICATORS:

Slope (Rise/#ofPoints), Download Status, Waveform Plot

FRONT PANEL:

This version has the title “AGLIENT LOAD WAVEFORM” written in black on a green background.

NORMAL OPERATION:

Run from “NMR Load Sweep.vi”.

DIAGRAM:

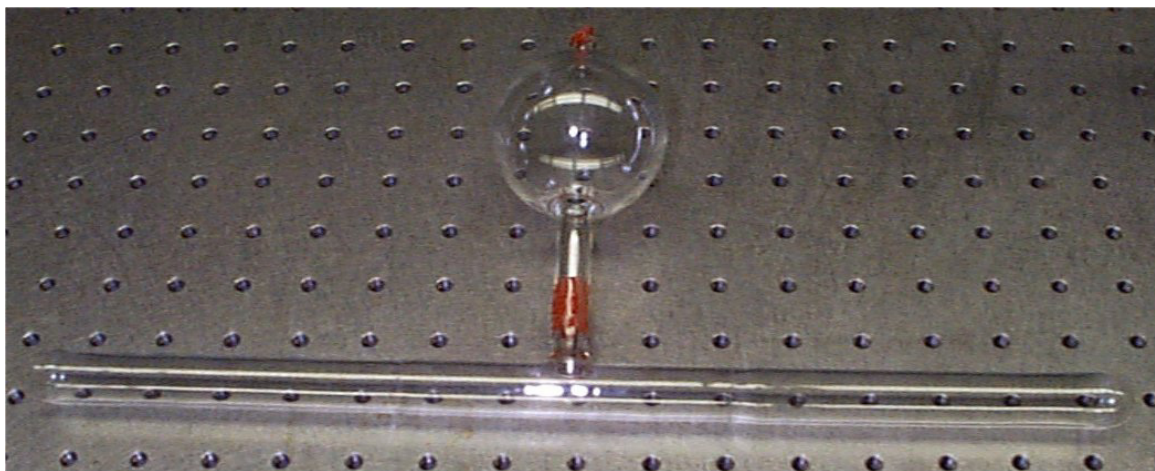
Frame	Description
Outside Left	Upper box shows initializations (Download status, y-intercept) and indicator declarations. Below and to the left is a calculation of the number of points needed for the ramp up/down and the sit time. *Important* Since this may or may not divide evenly, it is useful to select 15999 points (and not 16000) to ensure that enough points are available for the waveform. The slope of the ramp is also calculated.

0 Lower	The number of ramp points is calculated
1 Lower	The ramp points are defined using a for loop. These values are collected in an array “RAMP UP”.
2 Lower	The sit points are defined using a for loop. These values are collected in an array “SIT”.

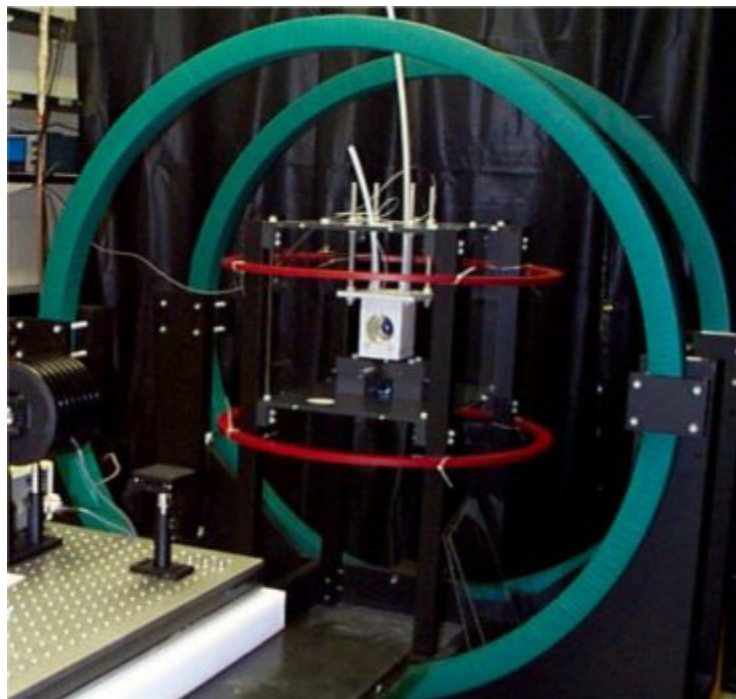
Outside Right	The RAMP UP array is copied and reversed into the RAMP DOWN array. The RAMP UP, RAMP DOWN, and SIT arrays are combined, plotted, and changed into text strings for the function generator command.
---------------	--

True	
0 Upper	The values of all the data points are sent to the FG. This may take several minutes so the timeout is disabled.
1 Upper	This data is copied from volatile memory to the waveform “NMR_WAVE”
2 Upper	Download Complete!

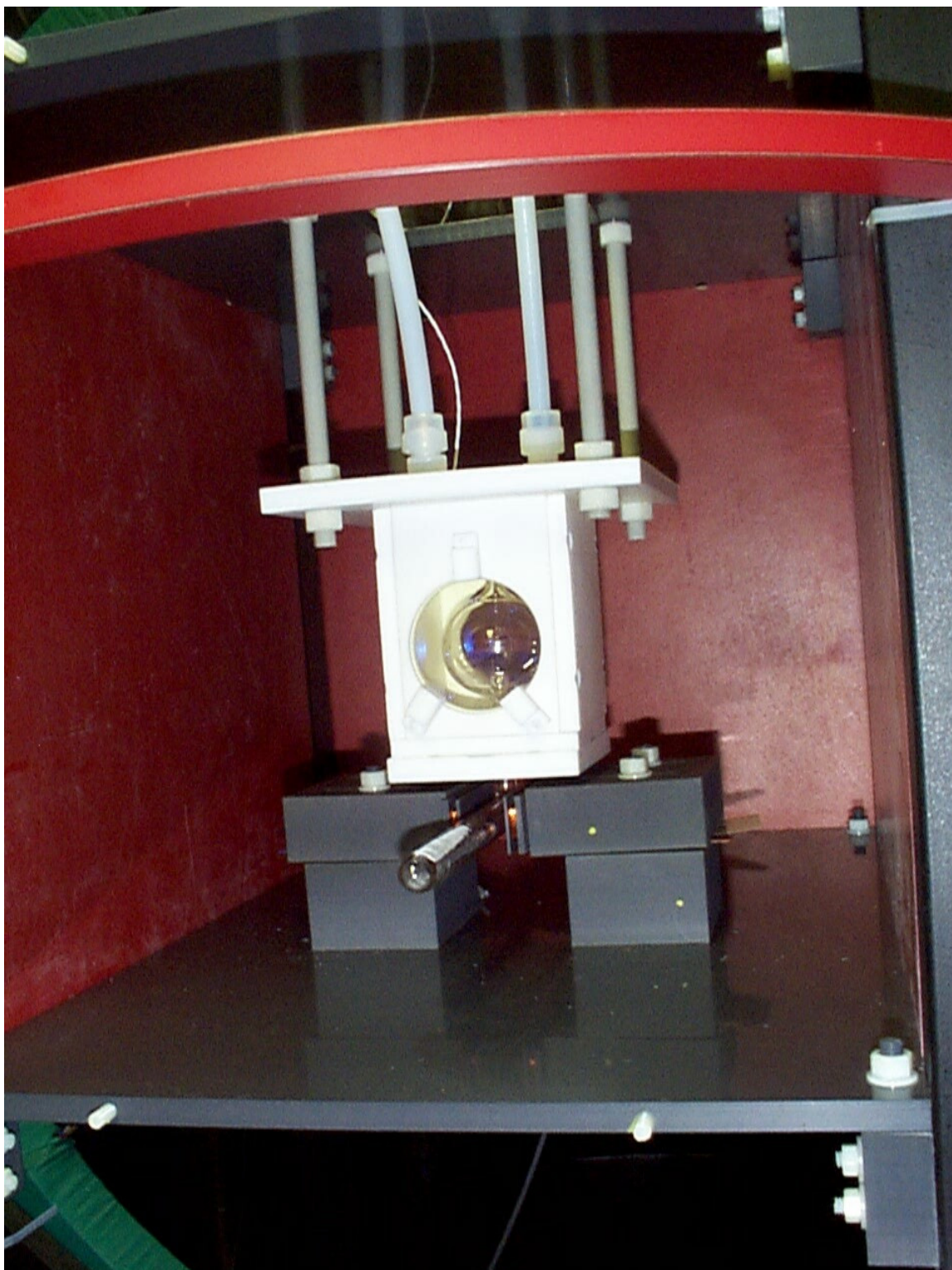
APPENDIX B - PICTURES



Picture 1: A ${}^3\text{He}$ target cell.



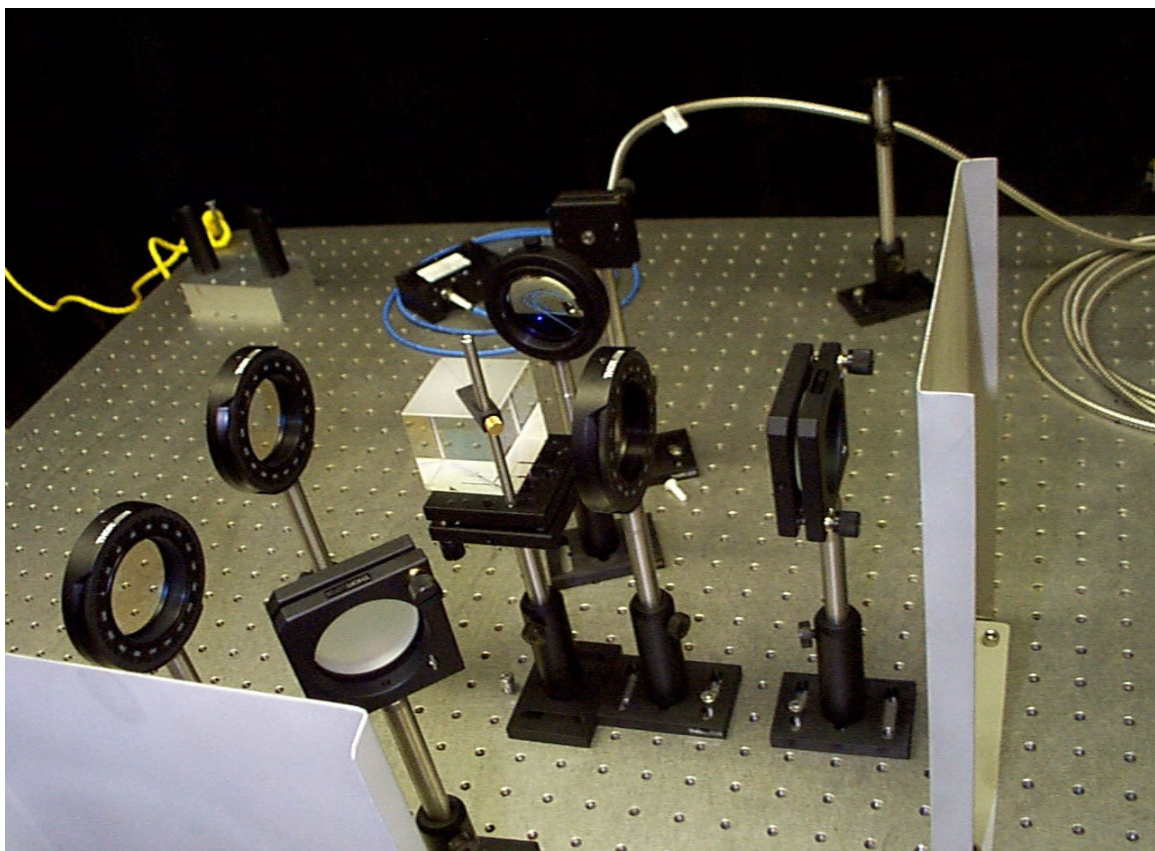
Picture 2: The NMR system including the main coils (outer pair), RF coils (inner pair), and oven (center).



Picture 3: The oven with target cell mounted and pickup coils aligned alongside the cell.



Picture 4: A side view of a pickup coil.



Picture 5: The optics setup. Light from the laser is directed through the optical fiber at the upper right to the stand at the top. The beam travels through the optics and then out to the target (off left).

REFERENCES

-
- [1] J.D. Bjorken, Phys. Rev. D **1**, 1376 (1970).
 - [2] S.D. Drell, A.C. Hearn, Phys. Rev. Lett. **16**, 908 (1966); S.B. Gerasimov, Sov. J. Nucl. Phys. **2**, 430 (1966).
 - [3] B.G. Yerozolimsky, Nucl. Instr. and Meth. in Phys. Res. A **440**, 491 (2000).
 - [4] J.R. Johnson *et al.*, Nucl. Instr. and Meth. in Phys. Res. A **356**, 148 (1995).
 - [5] R.M. Woloshyn, Nucl. Phys. A **496**, 749 (1989).
 - [6] G. Cates and Z.-E. Meziani, Thomas Jefferson National Accelerator Facility Proposal E94-101, <http://hallaweb.jlab.org/physics/experiments/he3/>
 - [7] H. Gao, Thomas Jefferson National Accelerator Facility Proposal E95-001, <http://hallaweb.jlab.org/physics/experiments/he3/>
 - [8] Z.-E. Mezinai, Thomas Jefferson National Accelerator Facility Proposal E99-117, <http://hallaweb.jlab.org/physics/experiments/he3/>
 - [9] T. Averett and W. Korsch, Thomas Jefferson National Accelerator Facility Proposal E97-103, <http://hallaweb.jlab.org/physics/experiments/he3/>
 - [10] P.L. Anthony *et al.*, Phys. Rev. Lett. **71**, 959 (1993).
 - [11] J.-P. Chein, Neutron Spin Structure Study at Jefferson Lab Hall A, (2002) to be published in Int. J. of Mod. Phys. A,
<http://hallaweb.jlab.org/physics/experiments/he3/A1n/talk/pacific-spin2001-jpchen.ps>
 - [12] E.E. de Lange *et al.*, Radiology **210**, 851 (1999).
 - [13] H.E. Möller *et al.*, Magnetic Resonance in Medicine **45**, 421 (2001).
 - [14] M.S. Albert *et al.*, Nature **370**, 199 (1994).
 - [15] Radiology Department - Hyperpolarized Gases Research -- UVA Health System,
<http://imaging.med.virginia.edu/hyperpolarized/background.htm>, 2001.
 - [16] Radiology Department - Hyperpolarized Gases Research -- UVA Health System,
<http://imaging.med.virginia.edu/hyperpolarized/current.htm>, 2001.

-
- [17] J.L. Knowles, Investigation of Techniques for Producing High Polarization ^3He Gas Targets, College of William and Mary, (1999).
 - [18] M.V. Romalis, Laser polarized ^3He target used for a precision measurement of the neutron spin structure, Princeton University, (1997).
 - [19] T.G. Walker, W. Happer, Rev. Mod. Phys. **69**, 629 (1997).
 - [20] N.R. Newbury, A.S. Barton, G.D. Cates, W. Happer, and H. Middleton, Phys. Rev. A **48**, 4411 (1993).
 - [21] K.D. Bonin, T.G. Walker, and W. Happer, Phys. Rev. A **37**, 3270 (1988).
 - [22] K.D. Bonin, D.P. Saltzberg, and W. Happer, Phys. Rev. A **38**, 4481 (1988).
 - [23] K.P. Coulter, A.B. McDonald, G.D. Cates, W. Happer, and T.E. Chupp, Nucl. Instr. Meth. A **276**, 29 (1989).
 - [24] I. Kominis, Measurement of the Neutron (^3He) Spin Structure at Low Q^2 and the Extended Gerasimov-Drell-Hearn Sum Rule, Princeton University, (2001).
 - [25] G.D. Cates, S.R. Schaefer, and W. Happer, Phys. Rev. A **37**, 2877 (1988).
 - [26] G.D. Cates, D.J. White, T.R. Chien, S.R. Schaefer, and W. Happer, Phys. Rev. A **38**, 5092 (1998).
 - [27] J.E. Mellor, Investigation of a Sol-Gel Coating Technique for Polarized ^3He Target Cells, College of William and Mary, (2001).
 - [28] A. Abragam, Principles of Nuclear Magnetism, Oxford University Press, 1999.
 - [29] Lide, D.R., Ed., CRC Handbook of Chemistry and Physics 82rd Ed., CRC Press, Boca Raton, FL, 2001.
 - [30] J. G. Powles, Proc. Phys. Soc., **71**, 497-500, 1958.